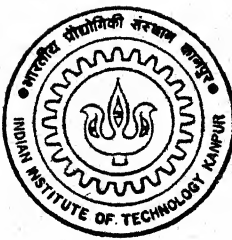


GEOMETRIC MODELING OF SINGLE POINT AND FLUTED TOOL SURFACES

by

Yogesh V. Deo



**ME
1997
M
DEO
GEO**

DEPARTMENT OF MECHANICAL ENGINEERING

Indian Institute of Technology Kanpur

AUGUST 1997

**GEOMETRIC MODELING
OF
SINGLE POINT AND FLUTED TOOL SURFACES**

A Thesis Submitted
in Partial Fulfilment of the Requirements
for the Degree of
MASTER OF TECHNOLOGY

by

Yogesh V. Deo

to the

**DEPARTMENT OF MECHANICAL ENGINEERING
INDIAN INSTITUTE OF TECHNOLOGY KANPUR**

August, 1997

5 DEU 1997

CENTRAL LIBRARY
I.I.T., KANPUR

No. A 124439



A124439

ME-1997-M-DEO-GEO

Dedicated to

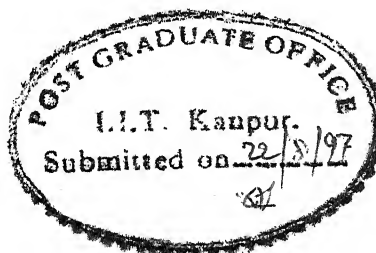
Aai and Dada

CERTIFICATE

It is certified that the work contained in the thesis entitled "Geometric Modeling of Single Point and Fluted Tool Surfaces", by "Yogesh V. Deo", has been carried out under my supervision and that this work has not been submitted elsewhere for a degree.

August, 1997

Dhande
Dr. Sanjay G. Dhande 21-8-97
Professor, ME and CSE
IIT Kanpur



Acknowledgements

I take this opportunity to express my deep gratitude to **Dr. Sanjay G. Dhande**. He was not only my guide; he is my mentor as well. Whenever I was in trouble, he was there to help me. His constant encouragement and invaluable guidance has led to the successful completion of the work. I remain grateful to him forever.

I am thankful to A.Rajarathinam for the valuable discussions I had with him and making my stay in CAD-P memorable.

I am thankful to all my friends especially B.Kumaraswamy, Rakesh, Tarun, Awadhesh, Siddharth, Hall 4 F-top friends and also Mr. A.D. Bhatt and Sanat Agrawal who made my stay comfortable and enjoyable at I.I.T kanpur.

I would like to thank CAD-P lab staff, who helped me in one way or other.

Yogesh Deo

Table of Contents

Title Page	i
Certificate	ii
Acknowledgements	iii
Table of contents	iv
List of Figures	v
List of Symbols	vi
Abstract	viii
 1. Introduction	 1
1.1 Geometric Modeling - A Review	
1.2 Specifications of the Tool Geometries	3
1.2.1 Single Point Cutting Tool	3
1.2.2 Twist Drill	7
1.2.3 Ball End-mill	7
1.3 Statement of the Problem	9
1.4 Literature Review	9
1.5 Scope and Organization	10
 2. Relationship Between Geometric Representations of a Single Point Cutting Tool	
2.1 Introduction	12
2.2 Geometric Modeling of a Single Point Cutting Tool	12
2.3 Correction in Inverse Formula	15
2.4 Grinding Principle	16
2.5 Grinding the Principle Flank of a Single Point Cutting Tool	18
2.6 Grinding the Rake Face of a Single Point Cutting Tool	21

2.7 Interrelationship between the Three Systems	23
3. Geometric Modeling of Helical Flutes	25
3.1 Introduction	
3.2 Geometric Definitions of helical paths	25
3.2.1 Cylinder	25
3.2.2 Cone	27
3.2.3 Hemisphere	27
3.2.4 Cylinder and Hemisphere	29
3.3 Section Geometry of the Fluted Tool	29
3.4 Fluted Surface Definition of Shank	29
3.5 End Surface Geometry	31
3.6 Integrated Tool Geometry	33
3.7 Derivation of the Cross-sectional Profile	35
4. Grinding of Fluted Tools	37
4.1 Grinding of Cutting Tools	37
4.2 Rake Face Grinding	39
4.3 Clearance Face Grinding	43
4.4 Some Observations	45
5. Conclusions	46
5.1 Summary of Technical Work	46
5.2 Suggestions for Further Work	47
References	51
Appendix	53
A. Transformations	53

List of Figures

Figure 1.1	Geometric Model for Shape Representation	2
Figure 1.2(a)	Tool in Hand Nomenclature	4
Figure 1.2(b)	Nomenclature of ASA System	4
Figure 1.2(c)	Nomenclature of ORS System	6
Figure 1.2(d)	Nomenclature of NRS System	6
Figure 1.2(e)	Nomenclature of MRS System	8
Figure 1.3	Twist Drill	8
Figure 1.4	Ball End-mill	10
Figure 2.1(a)	Modeling the Auxiliary Flank	13
Figure 2.1(b)	Modeling the Principle Flank	13
Figure 2.2	Grinding Priciple	17
Figure 2.3(a)	Isometric View of Principle Flank	17
Figure 2.3(b)	Projections of Normal of Principle Flank	19
Figure 2.3(c)	Grinding of Principle Flank	19
Figure 2.4(a)	Projections of Normal of Rake Face	22
Figure 2.4(b)	Grinding of Rake Face	22
Figure 2.5	Interrelationship Between Three Systems	22
Figure 3.1(a)	Helical Path along Cylinder	28
Figure 3.1(b)	Helical Path along Cone	28
Figure 3.1(c)	Helical Path along Hemisphere	28
Figure 3.1(d)	Helical Path along Cylinder and Hemisphere	30
Figure 3.2	Cross-sectional Geometry of Four Fluted Tool	30
Figure 3.3	Surface Model of End-mill with Ball End	32
Figure 3.4	Surface Model of End-mill with Conical End	34
Figure 4.1(a)	Five-axis Walter Helitronic Power CNC Tool Grinder	38
Figure 4.1(b)	Six-axis Ewamatic 106 CNC Tool Grinder	38

Figure 4.1(c)	Five-axis Huffman HS 155 CNC Tool Grinder	38
Figure 4.2	Grinding of Rake Face	40
Figure 4.3	Grinding of Clearance Face	44
Figure 5.1	End-mill with Ball End	48
Figure 5.2	End-mill with Conical End	48
Figure 5.3	Extruder Screw	49
Figure 5.4	Extruder Screw	49
Figure 5.5	Rapid Prototype Model of Extuder Screw	50
Figure 5.6	Rapid Prototype Model of Extuder Screw	50

List of Symbols

Single Point Cutting Tool

α_1	Rotational angle for auxiliary flank about the X-axis
α_2	Rotational angle for principal flank about the X-axis
α_3	Rotational angle for rake face about the X-axis
α_n	Normal clearance angle on the principle flank
α'_n	Normal clearance angle on the auxiliary flank
α_o	Orthogonal clearance angle on the principle flank
α'_o	Orthogonal clearance angle on the auxiliary flank
α_x	Side clearance angle on the principle flank
α_y	End clearance angle on the principle flank
α'_x	Side clearance angle on the auxiliary flank
α'_y	End clearance angle on the auxiliry flank
β_1	Rotational angle for auxiliary flank about Y- axis
β_2	Rotational angle for principal flank about Y- axis
γ_3	Rotational angle for rake face about Z- axis
γ_m	Maximum rake angle
γ_n	Normal rake angle
γ_o	Orthogonal rake angle
γ_s	Side rake angle
γ_b	Back rake angle
λ	Inclination angle
Φ	Principal cutting edge angle
Φ_e	End cutting edge angle
Φ_s	Side cutting edge angle
Φ_y	Angle of maximum rake plane with transverse direction
r	Nose radius

Fluted Tools

R	Radius of shank
H	Lead of helix
$r(z)$	Radius of ball at distance z
p	Pitch of the helix
α_1	Primary clearance angle
α_2	Secondary clearance angle
α_3	Rake angle
l_1	Primary clearance land width
l_2	Secondary clearance land width
l_3	Rake land width
r_1	Flute radius
r_2	Fillet radius
r_3	Flute radius
θ_{end}	End angle for ball part

Abstract

Cutting tool surfaces are either planar or doubly-curved surfaces. Conventionally, such surfaces were represented by means of a set of cross-sectional profiles. However, the techniques of Computer Aided Geometric modeling provide a unified representation of the cutting tool surfaces. In the present work, geometric models of single point as well as fluted cutting tool surfaces have been explored. In particular, the fluted surfaces have been represented as helicoidal surfaces.

Inverse and forward relationships between different nomenclatures of geometry of a single point cutting tool and the biparametric surface representations of the different faces of the same tool. The problem of providing the appropriate data of the orientation of a grinding wheel for grinding different surfaces such as rake surface and clearance surfaces has been investigated in the present work. Using the condition that the normal of the grinding surface should be collinear with the normal of the cutting tool surface, it has been found that the necessary data for grinding operation can be obtained.

The present work includes the development of suitable CAD software for geometric modeling of fluted cutting tool surfaces. The geometric models have been verified by realizing the cutting tool using the Rapid Prototyping Process. Specifically, the Fusion Deposition Modeling process has been used. The methodology developed has been illustrated by some numerical examples.

Chapter 1

Introduction

1.1 Geometric Modeling - A Review

The term geometric modeling refers to a collection of methods used to define the shape and other geometric characteristics of an object. It first came into use in the early 1970s with the rapidly developing computer graphics and computer aided design and manufacturing. Geometric modeling embraces an area often called computational geometry and extends beyond this to the newer field of solid modeling, creating an elegant synthesis of geometry and the computer.

Geometric modeling is the technique used to describe the shape of an object. Physical realizability of a designed shape is a primary concern of any manufacturing activity. If the surface is to be realized using a milling like process then it is necessary to select the most appropriate geometry of the cutting tool as well as the most suitable kinematic structure of the machine tool or the machining center. In some cases, a manufacturing engineer may have alternative options of cutting tool geometries and machine tool structures available for realizing a given designed surface. In such a case, it is necessary to find, before hand, the most appropriate combination of a machine tool type and cutting tool geometry. Furthermore, a manufacturing engineer is usually called upon to define the law of relative motion between the cutting tool and the blank for a given type of kinematic structure of the machine tool. This is necessary since many machines are now being controlled using CNC controllers. All such problems can be solved using geometric modeling methods. Geometric modeling makes possible process planning, design of tolerances, design for reliability, testability and maintainability (Figure 1.1.)

Geometric modeling provides a description of the model that is analytical, mathematical and abstract rather than descriptive. A geometric model is created because it is convenient and economical to substitute for the real object or the process. It is often lot easier to analyze the model rather than to test or measure or experiment with the real object. The three most important aspects of geometric modeling are,

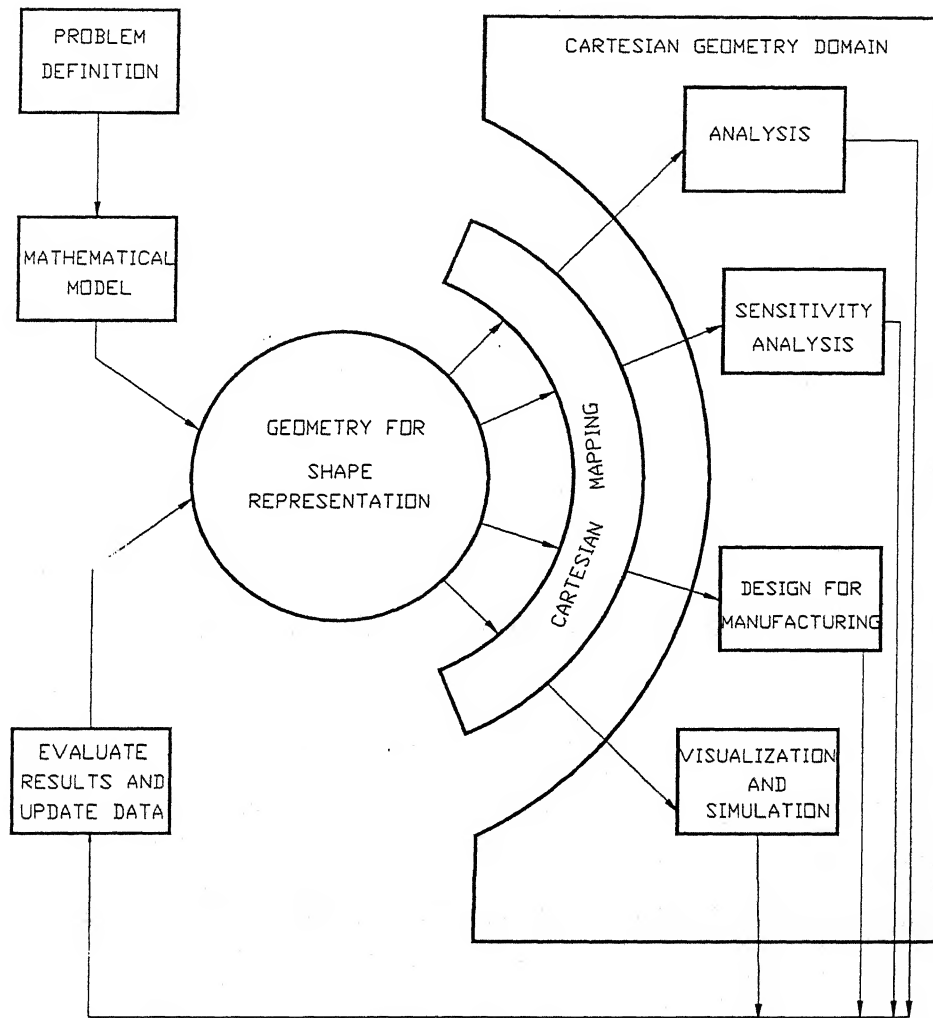


Figure 1.1 Geometric Model for Shape Representation

- **Representation** : The physical shape of an object is given and presumed to be fixed, compute a mathematical approximation.
- **Design** : To create a new shape to satisfy some operational or aesthetic objectives. To manipulate the variables defining the shape until the objectives are met.
- **Rendering** : This involves getting the image of the model in rendered form on the computer to be able to visualize it.

These three aspects are very closely interlinked.

In the present work, a mathematical model of the complex geometry of the ball-end mill and the other tools is formulated as a combination of the surfaces using the concept of computational geometry. Also the setting angles required for the sharpening of a single point cutting tools are found out. A geometric model defining the interrelationship between the three systems of a single point cutting tool for grinding, is formulated.

1.2 Specifications of the Tool Geometries

1.2.1 Single Point Cutting Tool

The geometry of a single point cutting tool consists of the following elements: face or rake surface, flank, cutting edges and the corner. Face is the surface of the cutting tool along which the chips flow out. Flank surfaces are those facing the workpiece. There are two flank surfaces, principal and auxiliary. Principal cutting edge performs the major portion of cutting and is formed by the intersecting line of the face with the principal flank surface. Auxiliary cutting edge (end cutting edge) is formed by the intersection of the rake surface with the auxiliary flank surface. The corner point is the intersection point of the principal cutting edge with the auxiliary cutting edge. The tool-in-hand nomenclature of a single point turning tool is shown in Figure 1.2(a).

Single Point Cutting Tools and their Nomenclatures

The geometry of most of the cutting tools have been developed on the basis of experience rather than analysis and experiments, using the various methods of specifying the tool geometry. Some of the important standards as far as the geometry of single point cutting tools are concerned are,

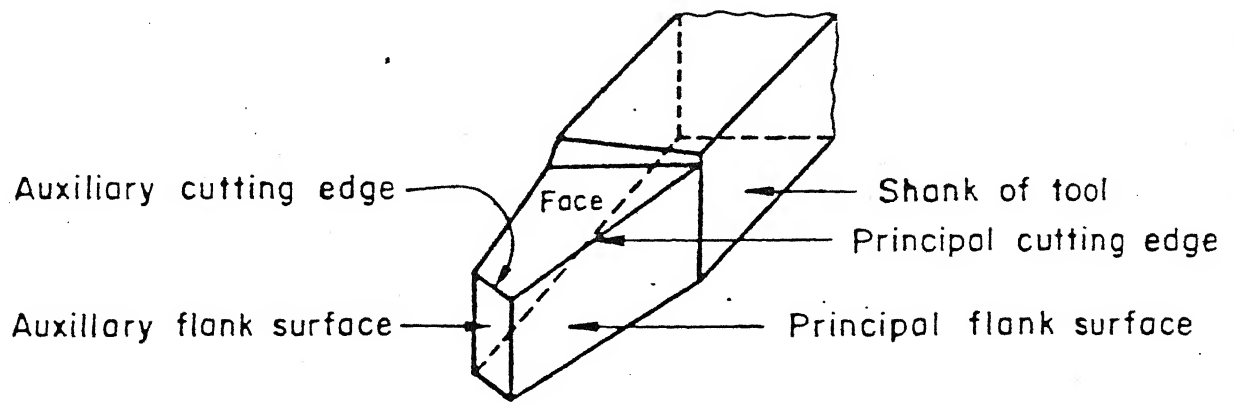


Figure 1.2(a) Tool in Hand Nomenclature

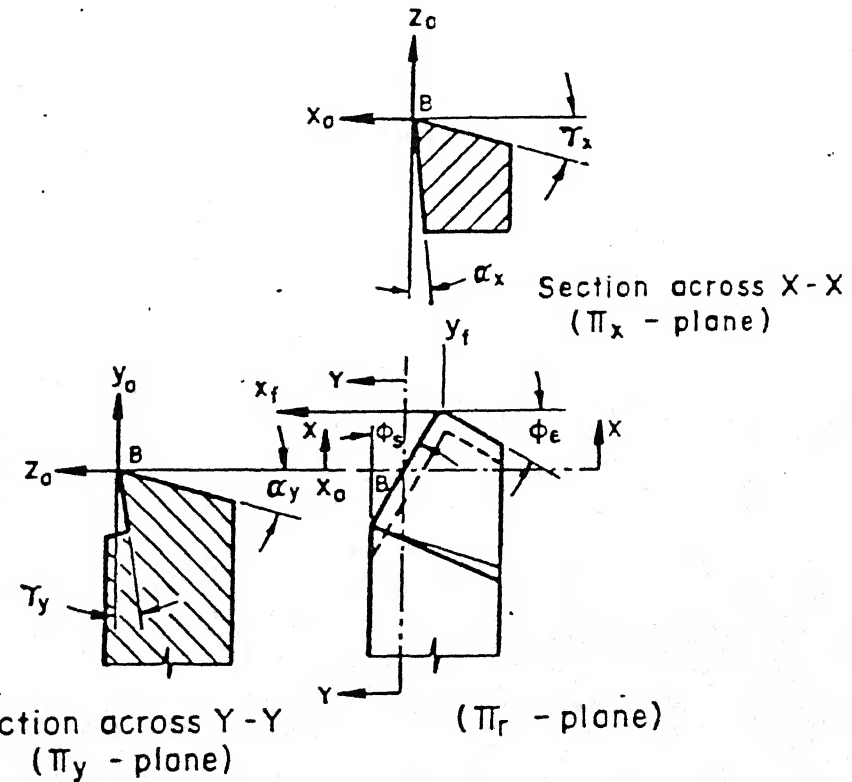


Figure 1.2(b) Nomenclature of ASA System

1) American Standards Association (ASA)

The ASA system is also called the Machine Reference System because the nomenclature is defined with respect to the standard machine movements.(Figure 1.2(b).)In this system the orientation of the rake face is defined by two rake angles, the back rake angle (Υ_y) and the side rake angle (Υ_x). The orientation of the principal flank is defined by the side clearance angle (α_x) and the end clearance angle (α_y).The auxiliary flanks also have the corresponding clearance angles denoted as ($\alpha_{x'}$) and ($\alpha_{y'}$) respectively. The cutting edge angle is defined by the side cutting edge angle (Φ_s) and the end cutting edge angle(Φ_e). The nose radius of the tool tip is r . The tool signature in this system is : $\Upsilon_y - \Upsilon_x - \alpha_y - \alpha_x - \Phi_e - \Phi_s - r$

2) Orthogonal Rake System (ORS)

This system is also called the Continental system. The important angle in this system are the side rake angle (Υ_o), which is also called the orthogonal rake angle and the back rake angle (λ), also called the inclination angle. The angles of the cutting edges are the principal cutting edge angle (Φ) and the end cutting edge angle (Φ_e).(Figure 1.2(b).)

The tool signature in this system is : $\lambda - \Upsilon_o - \alpha_o - \alpha_o' - \Phi_e - \Phi - r$

3) Normal Rake System (NRS)

This system is also called the ISO system. In this system the rake face is defined by two angles, the side rake angle (Υ_n) and the back rake angle (λ) which are also called the normal rake angle and inclination angle respectively. The other important angles are the clearance angles of the two flanks, the principal flank (α_n) and the auxiliary flank (α_n').The geometry of the cutting edges is specified by the principal cutting edge angle (Φ) and the end cutting edge angle (Φ_e) (Figure 1.2(c).)

The tool signature in this system is : $\lambda - \Upsilon_n - \alpha_n - \alpha_n' - \Phi_e - \Phi - r$

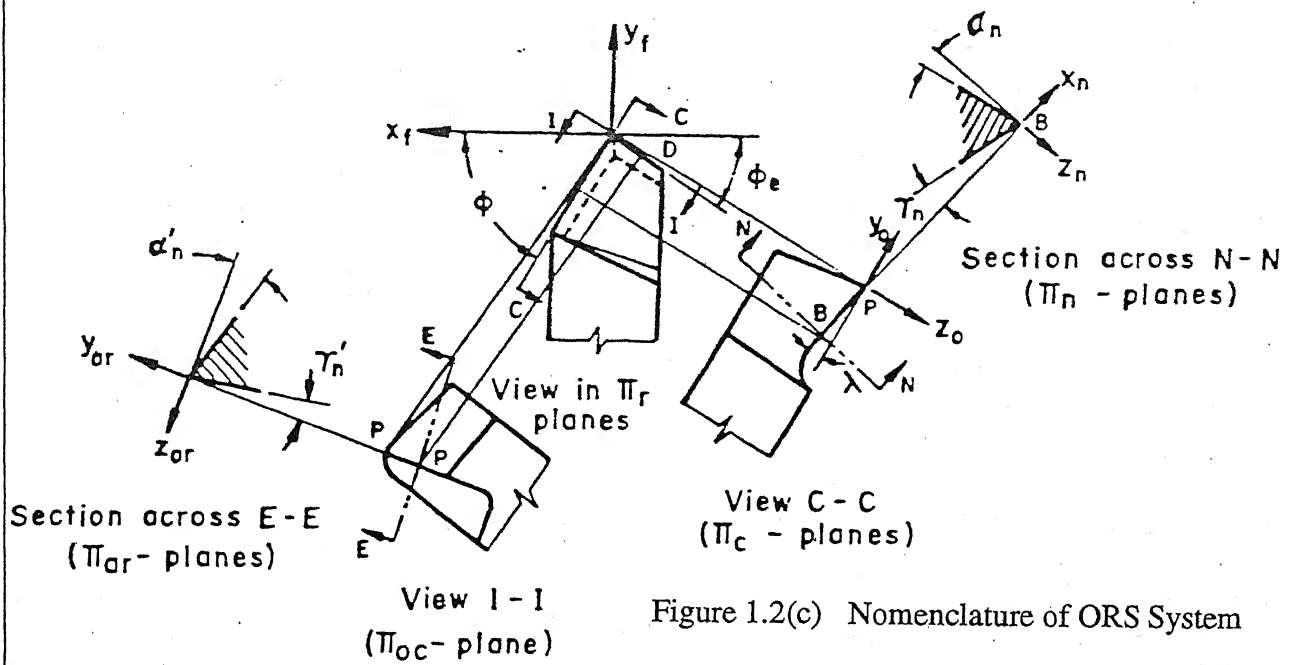


Figure 1.2(c) Nomenclature of ORS System

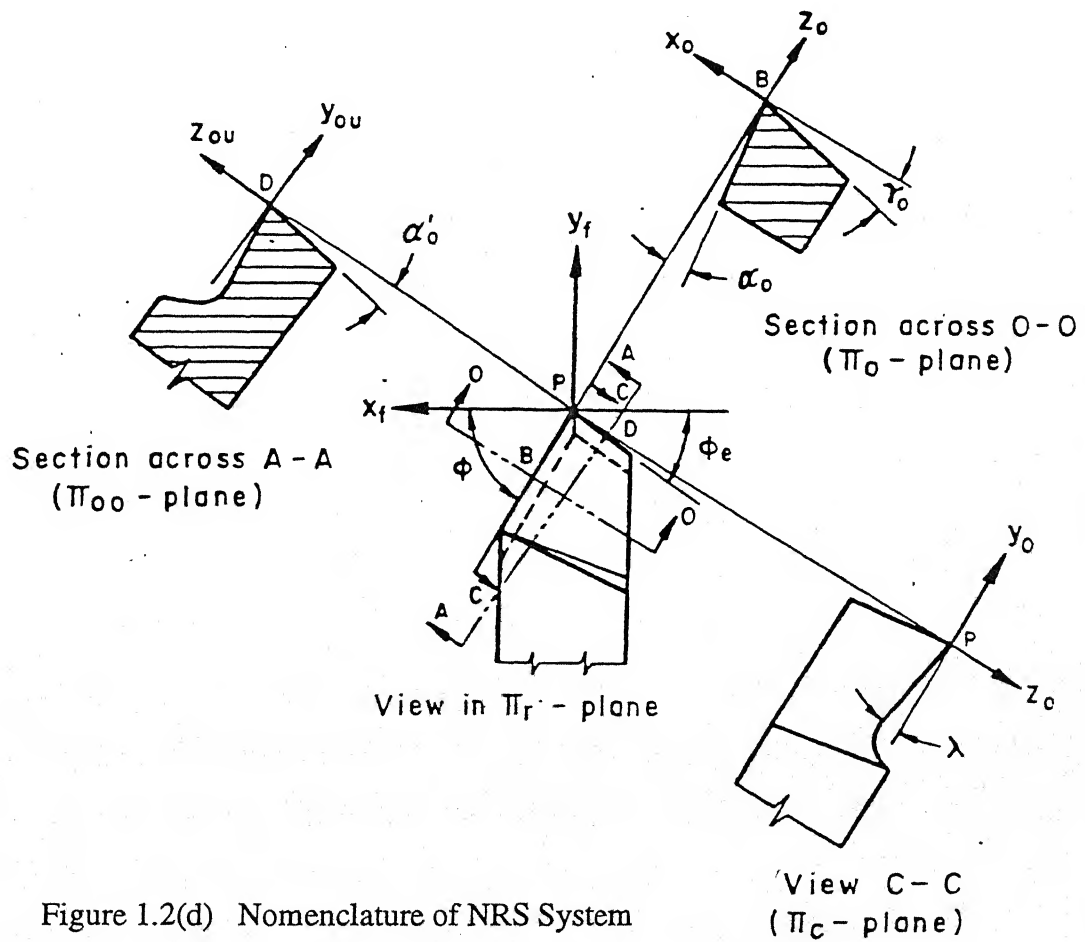


Figure 1.2(d) Nomenclature of NRS System

4) Maximum Rake System (MRS)

This system is followed by the British Standards. The two important angles are the maximum rake angle (Y_m) and the inclination angle (Φ_y). The cutting edges are specified as the principal cutting edge angle (Φ) and the end cutting edge angle (Φ_e). The clearance angles in this system are (α_o) and (α_o').

The tool signature in this system is : $\Phi_y - Y_{\max} - \alpha_o - \alpha_o' - \Phi_e - \Phi - r$

1.2.2 Twist Drill

A single point twist drill with cutting edges and various angles is shown in Figure 1.3. The main cutting edge (lip) is formed by the intersection of the helical surface of a flute with the lip clearance surface. The chisel edge is formed by the intersection of the lip clearance surfaces. Cutting occurs on the chisel edge and the cutting tips and the chips generated, travel up the axis of the drill through the flute. The cutting tips here correspond to the cutting edge of single point tools. A section perpendicular to the cutting tip clearly indicates the rake and flank angles. The rake angle, however, varies along the cutting edge and is the largest at the periphery. The rake angle results primarily from the helix angle of the flute.

No cutting occurs on the drill periphery except very near the outer corners which may be considered as the auxiliary cutting edge. The diameter of the drill is decreased over a certain portion of its circumference leaving the land at the full diameter to support the drill against the hole. This reduces rubbing between the drill and the hole. The point angle between the cutting edges provide gradual entry for the drill in a similar manner as the principal cutting edge of a single point tool.

1.2.3 Ball End-Mill

The ball end-mill cutter is essentially composed of the ball part and the end mill part. The flute geometry is specified by the helix angle (β), radial rake angle (α_3), and two clearance angles, primary clearance angle (α_1) and the secondary clearance angle (α_2), (Figure 1.4.) The radius of the ball part is equal to the radius of cylindrical shaft of the cutter body. On the cylindrical portion of the ball end-mill, the flutes have constant helix angle.

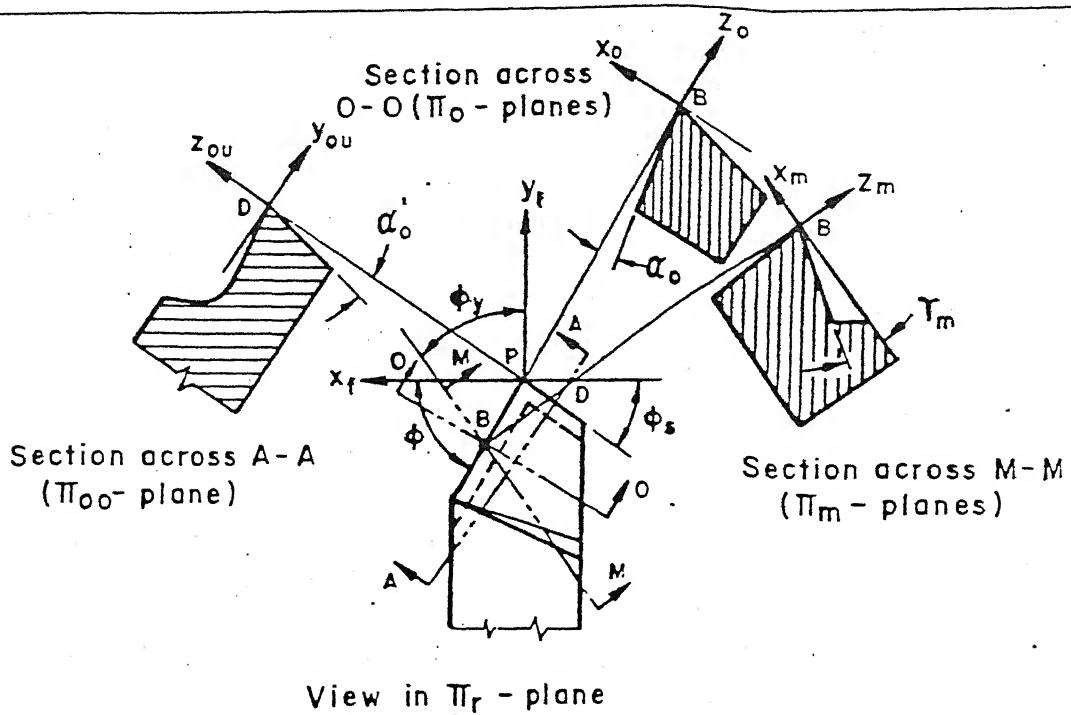


Figure 1.2(e) Nomenclature of MRS System

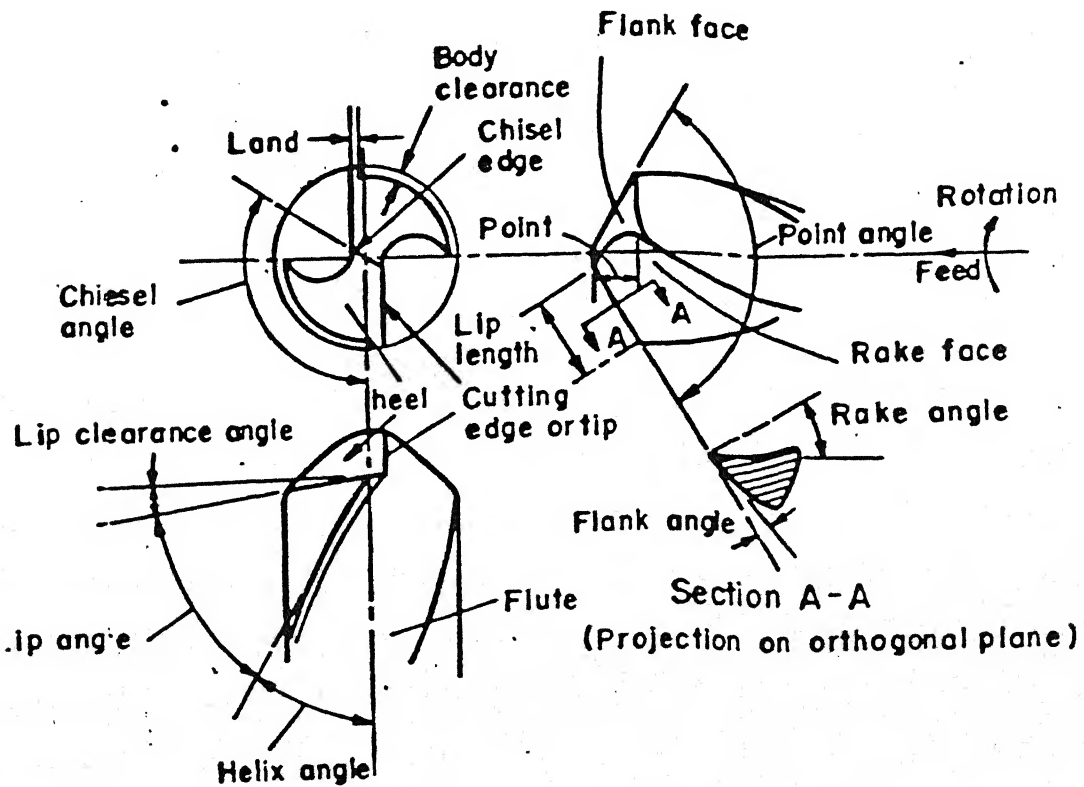


Figure 1.3 Twist Drill

On hemispherical portion the flutes have a constant lead, but have a varying local helix angle due to changing radius. And therefore rake angles are different along the flute of a ball end mill.

1.3 Statement of the Problem

The geometry of the twist drills has been studied extensively by the researchers, however the area of the ball end-mill cutter and the single point cutting tools has not received much attention. One of the reason for this could be the large variety of the tools that exist in actual practice. Thus to be able to create a comprehensive geometric model that could take into account this wide variety of tool geometry is rather difficult and this could be one of the reason that the researchers have not been attracted towards modeling them and the field remains largely unexplored.

The basic statement of the problem of the modeling of fluted surfaces and a single point cutting tool for grinding and sharpening would cover the following range of topics

- (1) To find the setting angles of a single point cutting tool with reference to the grinding wheel.(Tool and cutter grinder system)
- (2) To define the interrelationship among the three systems, namely conventional method, geometric modeling system (CAD approach) and tool and cutter grinder system.
- (3) To define the complete geometry of the ball end mill cutter.
- (4) To develop a software application which runs in AutoCAD environment and
- (5) To make Rapid Prototype models using FDM technology.

1.4 Literature Review

Tsai and Wu [12] have derived explicit surface relations for the flank contours and have shown that they can be expressed in terms of the grinding parameters. This methodology has been also used to calculate the shape of chisel edges and their relationship with the grinding parameters. In the paper by Lin, Kang, Ehmann [6], a new helical micro-drill geometry has been suggested. In this work, helicoidal surface of the drill flank has been modeled as the surface generated by the line generator of the grinding wheel that rotates about an axis while also translating along the drill axis.

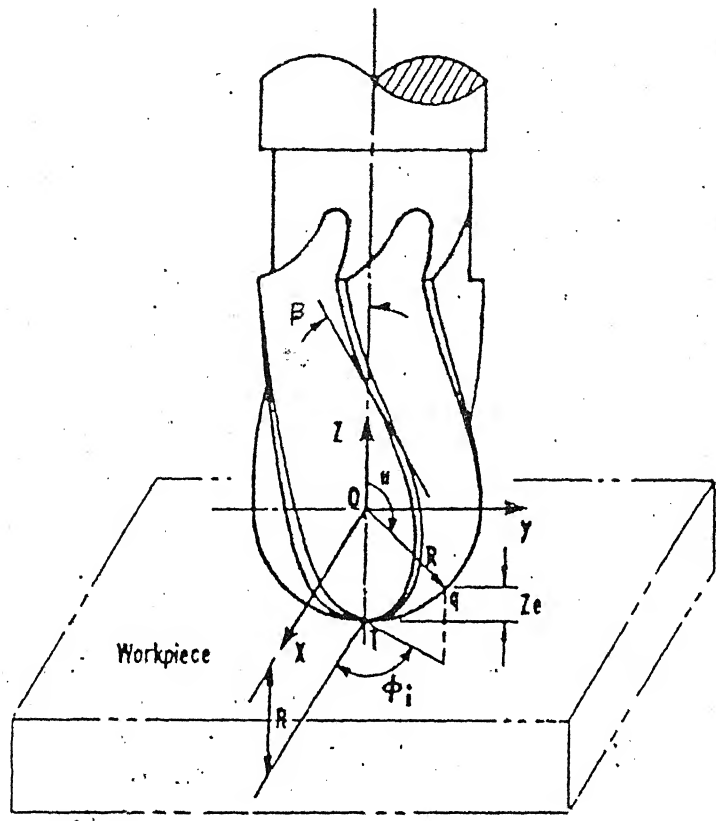


Figure 1.4 Ball End-mill

S.Fuji, M.F Devries and S.M Wu [5] have analyzed the optimum drill geometry for the conical drill. In this analysis the relationship between the drill design parameters and grinding parameters is established. These relationships have been used to design the drill and review its grinding.

Minyang Yang and Heeduck Park [14] analyzed the ball-end milling process, and its cutting force. Also they developed a model to predict the instantaneous cutting force on given machining conditions. Ching-Chih Tai and Kuang-Hua Fuh [11] studied a new predictive force model in ball-end milling using metal cutting theory and for the geometric relations of the ball-end milling process.

A general mechanics and dynamics model for helical end mills were studied by Y.Altintas and P.Lee [1].The general model allows prediction of cutting forces, dimensional surface errors for a class of helical end mills. Yucesan and Altintas [2] presented a model based on the analytical representation of ball shaped helical flute geometry and its rake and clearance surfaces.

T.S Rajpathak [9] has analyzed the geometric modeling of a single point cutting tool. Present work is in continuation of his work and also it includes the geometric modeling of the ball end-mill.

1.5 Scope and Organization

The scope of the thesis could be stated according to the following important points

- 1) To correct the inverse formula [9] used for finding the grinding angles.
- 2) To find the setting angles required for grinding and sharpening of a single point cutting tool.
- 3) To establish the relationship between the three systems, namely conventional system, geometric modeling system and tool and cutter system.
- 4) To define the helical path along different objects and to derive the cross-sectional geometry of a fluted shank.
- 5) To model the fluted surface along the end-mill portion and the ball part.
- 6) To develop a methodology for finding the setting angles required for grinding the fluted tools.
- 7) To make Rapid Prototype models of the ball end-mill and extruder screw using FDM technology.

The thesis is organized in the following manner.

Chapter 1 reviews the field of geometric modeling. Also it discusses the specifications of different tool geometries, such as single point cutting tool, twist drill and ball end-mill. Literature review is taken and the scope of present work is stated.

Chapter 2 discusses the method for finding the setting angles required for grinding and sharpening of a single point cutting tool. And it gives the relationship between the three systems of a single point cutting tool. Also in this chapter, the forward and inverse relationships between the systems of Nomenclature and the orientation angles of the geometrical surfaces constituting the cutting tool have been fully developed and verified.

Chapter 3 focuses on the development of the geometric model for the fluted cutting tools. One can mentioned the following examples of such cutting tools: twist drills, ball end-mills, flute end-mills, reamers, broachers etc. Such cutting tools provide cutting surfaces in the form of a set of helicoidal surfaces. The fluted channel is also a helicoidal surface. The geometric model proposed in the present work provides a mathematical representation which can be used for FEM analysis, generation of CNC data for grinding operations and design of cutting tools.

Chapter 4 discusses the methodology of grinding the cutting surfaces such as rake and clearance of the fluted cutting tools. These surfaces are ground using a grinding wheel, in the form of a frustum of a cone. The orientation of the grinding wheel requires that the grinding surface be orthogonal to the noraml vector of the helicoidal cutting surface. Such a condition can be accomplished using a tool and cutter grinder having five degrees of freedom.

Finally, **chapter 5** summarizes the accomplishments of the research efforts. Based on the work done so far, it has been felt that the field of Computer Aided Design of cutting tools can be developed using the concepts of geometric modeling and conjugate geometry. Suggestions for carrying out further work in this field have been described in chapter 5.

Chapter 2

Relationships Between Geometric Representations of a Single Point Cutting Tool

2.1 Introduction

In conventional system, the tool geometry of a single point cutting tool is described in either ASA, NRS, ORS or MRS system, as mentioned in Chapter 1. In this system, we get only two-dimensional geometry of the cutting tool. But the present need of the hour is to define the tool in three-dimensional geometry, as it is used for FEM analysis, stress analysis and simulation of the machining or grinding process. Therefore, it is necessary to establish the relationship between the conventional systems and the geometric modeling system of the tool.

Rajpathak[9] has done the work on the geometric modeling of the single point cutting tool. He also established the relationship between the conventional and the grinding angles. There were some discrepancies in the answers in the inverse relationship, which are corrected in the present work. Also in this work the setting angles required for grinding and sharpening of the tool are found out and the interrelationship between the three systems is established.

2.2 Geometric Modeling of a Single Point Cutting Tool

The basic methodology that has been developed [9] for the modeling of the tool considers the sharpening aspects as well as its manufacturing from an unmachined rectangular stock of the size $L \times B \times H$ where L is the length of the blank, B is the width of the blank and H is the height of the blank. The tool geometry is defined by six new angles, which are nothing but angular rotations of flat surfaces with reference to a fixed coordinate system.

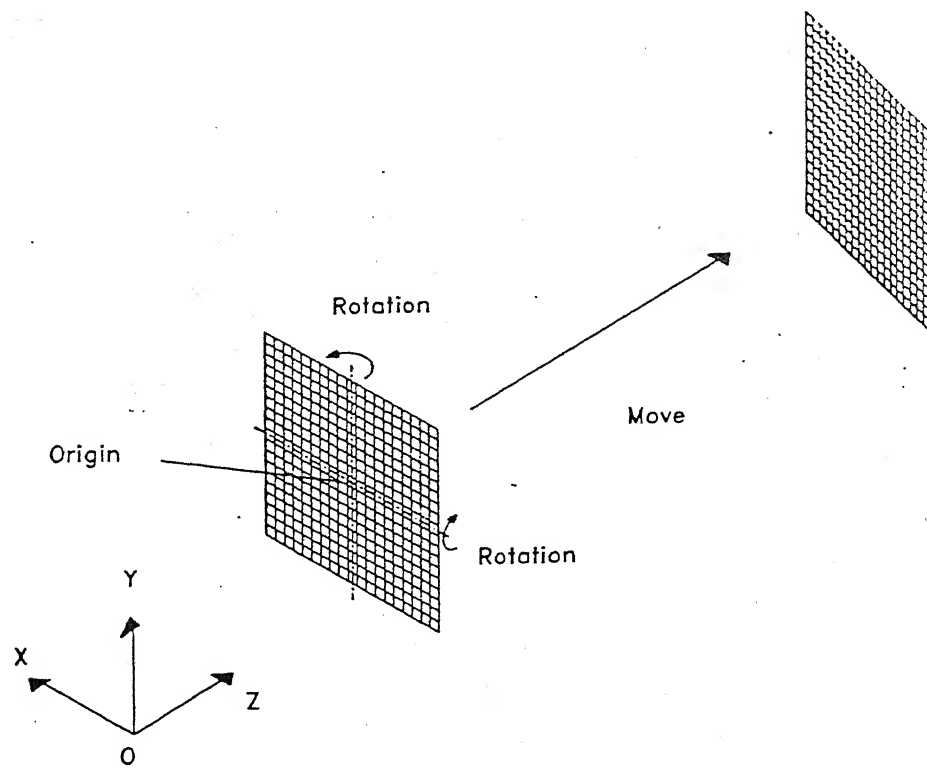


Figure 2.1(a) Modeling the Auxiliary Flank

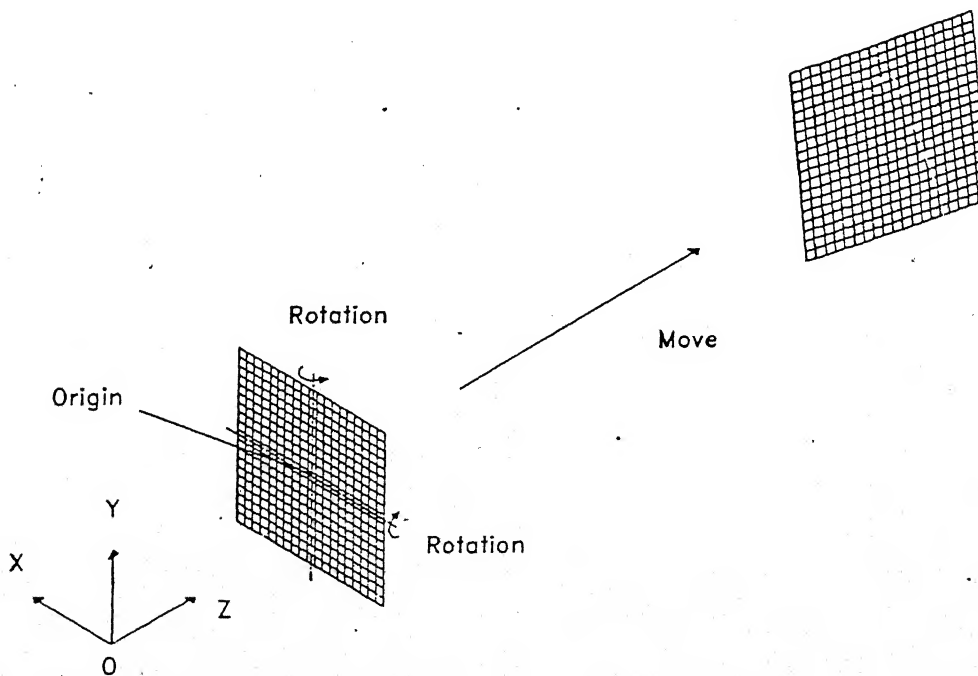


Figure 2.1(b) Modeling the Principle Flank

For example in order to position the auxiliary flank, the following transformations are to be successively applied to the plane, as per the auxiliary flank configuration of the tool.(Figure 2.1.)

- 1) Rotate the plane about the 'X' axis through angle ' α_1 '.
- 2) Rotate the plane about the 'Y' axis through angle ' β_1 '.
- 3) Translate the plane along the 'Z' axis through distance ' d_{13} '.

If qax , qay , qaz represents the transformed coordinates of any point on the plane then,

$$[qax \ qay \ qaz \ 1] = [u_1 \ v_1 \ 0 \ 1] [R_{x,\alpha 1}] [R_{y,\beta 1}] [T] \quad (2.1)$$

Performing the algebra in the equation as per the indicated rotations and the translation according to the transformation matrices in eqs (A2), (A5) and (A6), we get

$$qax = u_1 \cos \beta_1 + v_1 \sin \alpha_1 \sin \beta$$

$$qay = v_1 \cos \alpha_1$$

$$qaz = -u_1 \sin \beta_1 + v_1 \sin \alpha$$

where

$$(-\infty \leq u_1 \leq \infty)$$

$$(-\infty \leq v_1 \leq \infty)$$

Similarly the equation for the **principal flank** surface is given by,

$$[qpx \ qpy \ qpz \ 1] = [u_2 \ v_2 \ 0 \ 1] [R_{x,\alpha 2}] [R_{y,\beta 2}] [T] \quad (2.2)$$

And the equation for the **rake face** is given by,

$$[qrx \ qry \ qrz \ 1] = [u_3 \ 0 \ w_3 \ 1] [R_{z,\gamma 3}] [R_{x,\alpha 3}] [T] \quad (2.3)$$

2.3 Correction in the Inverse Formula

If the orientation angles ($\alpha_1, \beta_1, \alpha_2, \beta_2, \alpha_3, \gamma_3$) of the different faces of a single point cutting tool are given, we find the angles corresponding to the ASA Nomenclature ($\gamma_y, \gamma_x, \alpha_y, \alpha_x, \Phi_e, \Phi_s$) using forward formula. These angles of ASA Nomenclature are then substituted into the inverse relations [9] to find the grinding angles again. There was some discrepancy in the value of angle, found using inverse method as given by Rajpathak [9]. The correct value of the angle is found out as follows:

The clearance angles on the auxiliary flank are given by

$$\alpha'_y = \cos^{-1} \left[\frac{\cos \alpha_1 \cos \beta_1}{\sqrt{\sin^2 \alpha_1 + \cos^2 \alpha_1 \cos^2 \beta_1}} \right]$$

$$\alpha'_x = \cos^{-1} \left[\frac{-\cos \alpha_1 \cos \beta_1}{\sqrt{\sin^2 \alpha_1 + \cos^2 \alpha_1 \sin^2 \beta_1}} \right]$$

squaring both the equations we get,

$$\cos^2 \alpha'_y = \frac{\cos^2 \alpha_1 \cos^2 \beta_1}{\sin^2 \alpha_1 + \cos^2 \alpha_1 \cos^2 \beta_1} \quad (2.4)$$

$$\cos^2 \alpha'_x = \frac{\cos^2 \alpha_1 \sin^2 \beta_1}{\sin^2 \alpha_1 + \cos^2 \alpha_1 \sin^2 \beta_1} \quad (2.5)$$

let

$$c1 = \cos^2 \alpha'_y, \quad c2 = \cos^2 \alpha'_x$$

$$x = \cos^2 \alpha_1, \quad y = \cos^2 \beta_1$$

substituting these values in equation (2.1) and (2.2) we get

$$\begin{aligned} (1 - c1)xy + c1x - c1 &= 0 \\ (1 - c2)xy - x + c2 &= 0 \end{aligned} \quad (2.6)$$

Examples which will illustrate the correctness of the given equation (2.6) are given below.

Example 1

The grinding angles are

$$\alpha_1 = 5^\circ, \beta_1 = -15^\circ, \alpha_2 = 5^\circ, \beta_2 = 75^\circ, \alpha_3 = 6^\circ, \gamma_3 = 8^\circ.$$

With forward calculations and taking into account the sign conventions we get following angles :

$$\gamma_y = -6^\circ, \gamma_x = 8.045^\circ, \alpha_y = 18.6768^\circ, \alpha_x = 5.1754^\circ, \alpha'_y = 5.1754^\circ, \alpha'_x = 18.6768^\circ$$

When these values are substituted in the inverse formula, Rajpathak[9] got the following values:

$$\alpha_1 = 5^\circ, \beta_1 = -16.546^\circ, \alpha_2 = 5^\circ, \beta_2 = 75.117^\circ, \alpha_3 = 6^\circ, \gamma_3 = -8^\circ$$

Clearly, the example shows that there is discrepancy in the value of angle β_1 . With the method suggested above, for the same example we get the value of β_1 as -15.1041 .

Example 2

The grinding angles are

$$\alpha_1 = 5^\circ, \beta_1 = -13.964^\circ, \alpha_2 = 5^\circ, \beta_2 = 74.548^\circ, \alpha_3 = -8^\circ, \gamma_3 = 9.905^\circ.$$

With forward calculations and taking into account the sign conventions we get following angles :

$$\gamma_y = -8^\circ, \gamma_x = 10^\circ, \alpha_y = 18.1788^\circ, \alpha_x = 5.1865^\circ, \alpha'_y = 5.1515^\circ, \alpha'_x = 19.9283^\circ$$

When these values are substituted back in the inverse formula, Rajpathak[9] got the following values:

$$\alpha_1 = 5^\circ, \beta_1 = -15.619^\circ, \alpha_2 = 5^\circ, \beta_2 = 74.668^\circ, \alpha_3 = -8^\circ, \gamma_3 = 9.905^\circ$$

This example also shows the discrepancy in the value of angle β_1 . Solving the example with the help of equation (2.6), we get the value of β_1 as -13.9187 .

2.4 Grinding Principle

Most of the cutting tools are ground at the face and flank surfaces in order to impart the required stereometric features at the initial stage and also for resharpening the

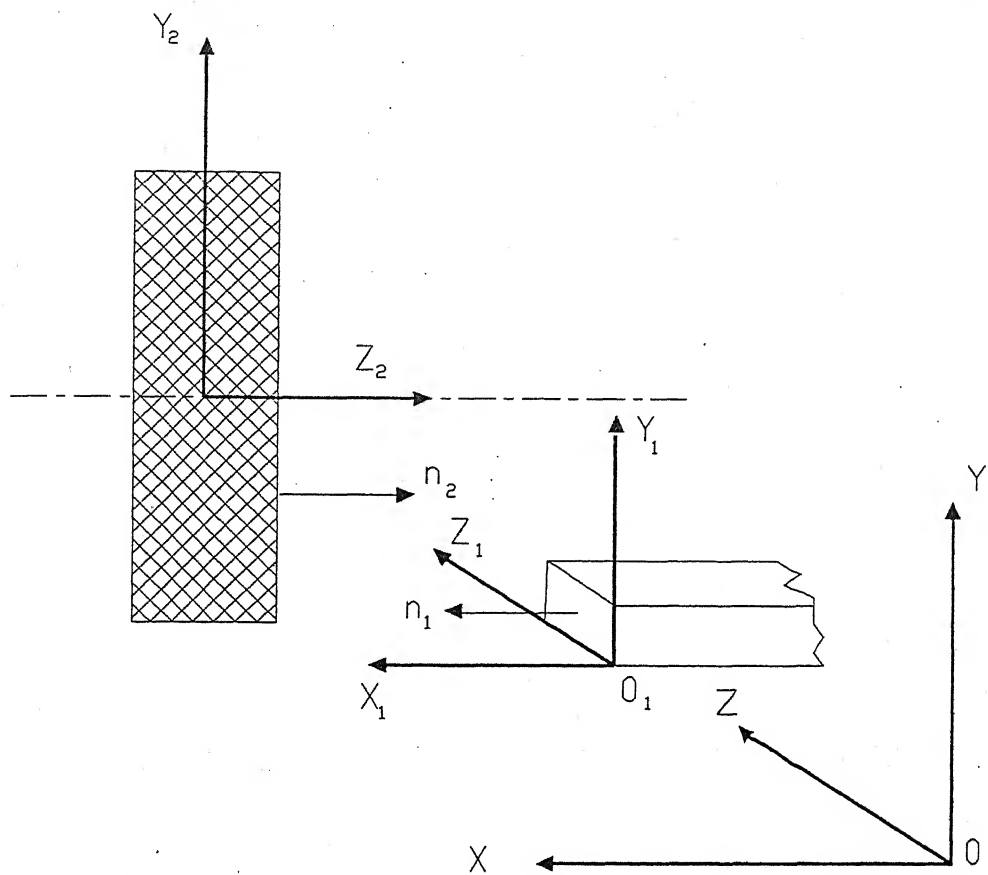


Figure 2.2 Grinding Principle

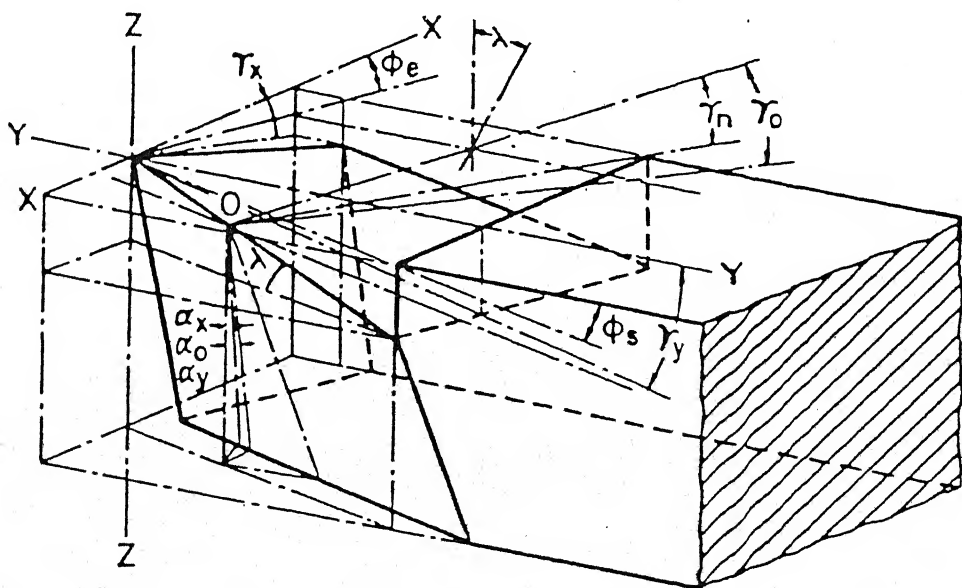


Figure 2.3(a) Isometric View of Principle Flank

features, so as to restore their machining capability. The elements to be ground may be flat, conical, spiral or helical in nature depending on the cutting tool like turning tool, drill, milling cutters etc. It is extremely important to orient the element to be ground with respect to the grinding wheel in order that the required element can be correctly ground.

As shown in Figure 2.2, let n_1 be the unit normal vector on the surface of the tool to be ground and n_2 be the unit normal vector acting on the grinding surface.

The condition for grinding is

$$n_1 = \pm n_2$$

With the change of settings, the direction of n_1 is altered. It is necessary to select that particular setting in which normal becomes perpendicular to the grinding face of the wheel. At this setting, the flat surface to be ground will be coincident with the grinding face and the specific feature can be reproduced through sharpening.

2.5 Grinding the Principal Flank of a Single Point Cutting Tool

Flank surfaces and rake face can be ground by several techniques employing either a three-dimensional attachment or with a swiveling work table. Here an attachment with three swivel setting is chosen for the analysis.

Figure 2.3(a) shows the isometric view of the principal flank and face surfaces of the single point cutting tool. The principal flank surface is described by two important angles α_x and α_y . Figure 2.3(b). In the vertical plane V, the clearance angle α_y is obtained, while in the profile plane P, the clearance angle α_x is determined. The projection of the normal n_1 acting on the actual flat surface to be ground are given by n_1' and n_1'' are perpendicular to the corresponding traces in the planes V and P.

In the initial setting, the tool is positioned such that the z_1 axis of the tool will become parallel to the axis of the grinding wheel. Figure 2.3(c).

In order to satisfy the grinding principle, the following transformations are performed on the tool successively

- 1) Rotation about 'Y' axis through angle ' θ_B '
- 2) Rotation about 'X' axis through angle ' θ_A '

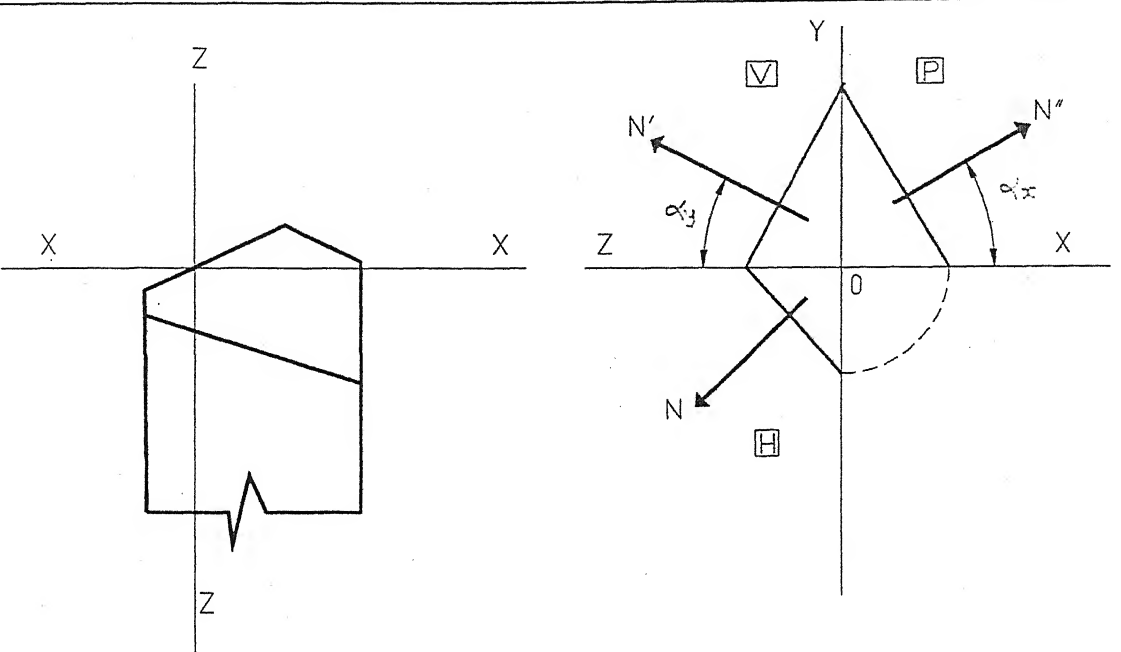


Figure 2.3(b) Projections of Normal of Principle Flank

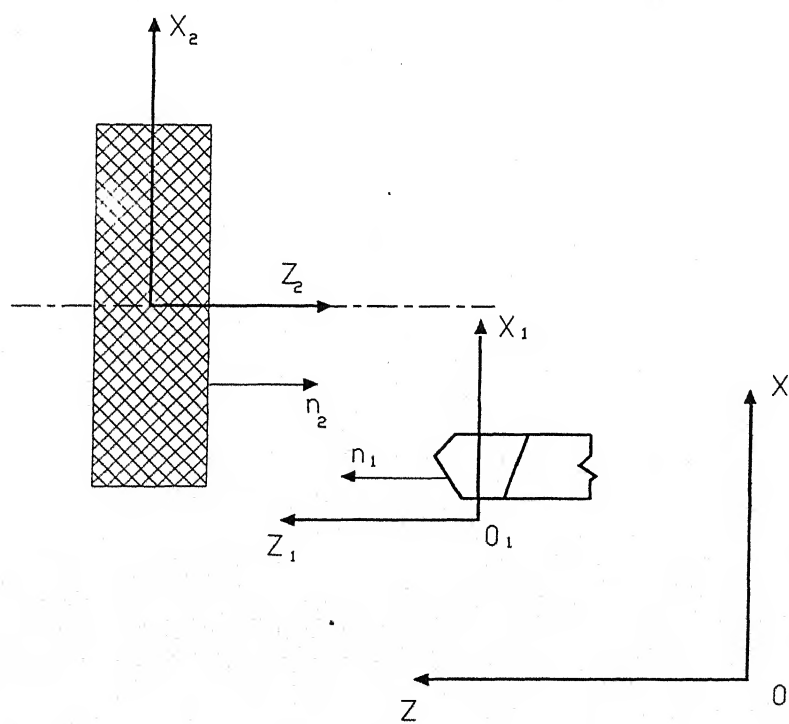


Figure 2.3(c) Grinding of Principle Flank

The equation is given as,

$$[n_2] = \pm [n_1] [R_{y,\theta_B}] [R_{x,\theta_A}] \quad (2.7)$$

Procedure to find the normal $[n_1]$ of the principal flank :

The equation of the principal flank surface is given by

$$\begin{aligned} qpx &= u_2 \cos \beta_2 + v_2 \sin \alpha_2 \sin \beta_2 \\ qpy &= v_2 \cos \alpha_2 \\ qpz &= -u_2 \sin \beta_2 + v_1 \sin \alpha_2 \end{aligned} \quad (2.8)$$

where,

$$(-\infty \leq u_2 \leq \infty)$$

$$(-\infty \leq v_2 \leq \infty)$$

Differentiating the above equation first with respect to u_2 and then with respect to v_2 and taking the cross product of it, we get

$$\frac{\partial R}{\partial u_2} \times \frac{\partial R}{\partial v_2} = \begin{vmatrix} i & j & k \\ \cos \beta_2 & 0 & -\sin \beta_2 \\ \sin \alpha_2 \sin \beta_2 & \cos \alpha_2 & \sin \alpha_2 \cos \beta_2 \end{vmatrix}$$

$$[n_1] = \begin{bmatrix} \cos \alpha_2 \sin \beta_2 \\ -\sin \alpha_2 \\ \cos \beta_2 \cos \alpha_2 \end{bmatrix}$$

$$[n_2] = \begin{bmatrix} 0 \\ 0 \\ 1 \end{bmatrix}$$

Substituting the above values in equation (2.7), we get

$$\begin{aligned}\theta_B &= -\beta_2 \\ \theta_A &= -\alpha_2\end{aligned}\quad (2.9)$$

Similarly for the auxiliary flank, solving the following equation

$$[n_2] = \pm[n_1][R_{y,\theta_B}][R_{x,\theta_A}] \quad (2.10)$$

we get

$$\begin{aligned}\theta_B &= -\beta_1 \\ \theta_A &= -\alpha_1\end{aligned}\quad (2.11)$$

2.6 Grinding the Rake Face of a Single Point Cutting Tool

Figure 2.4(a) shows the orientation of the normal N_1' and N_1'' in the vertical and profile projection planes. In the initial setup the tool is positioned such that the z_1 axis of the tool becomes perpendicular to the grinding wheel axis.

In order to satisfy the grinding principle, the following transformations are performed on the tool successively, (Figure 2.4(b))

- 1) Rotation about 'Y' axis through angle ' θ_B '
- 2) Rotation about 'X' axis through angle ' θ_A '

The equation is given as,

$$[n_2] = \pm[n_1][R_{y,\theta_B}][R_{x,\theta_A}] \quad (2.12)$$

Procedure to find the normal $[n_1]$ of the principal flank.

The equation of the rake face is given by

$$\begin{aligned}qr_x &= u_3 \cos \gamma_3 \\ qr_y &= u_3 \sin \gamma_3 \cos \alpha_3 - w_3 \sin \alpha_3 + d_{32} \\ qr_z &= u_3 \sin \gamma_3 \sin \alpha_3 + w_3 \cos \alpha_3\end{aligned}\quad (2.13)$$

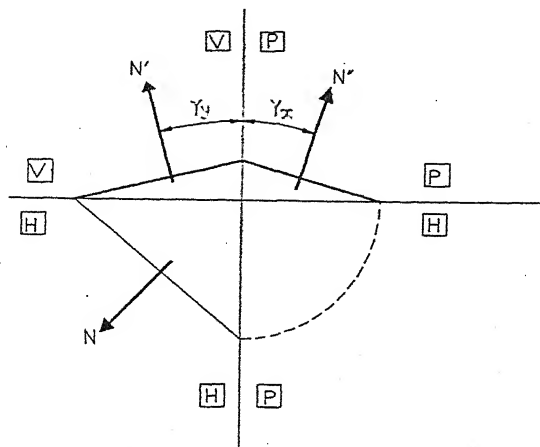


Figure 2.4(a) Projections of Normal of Rake Face

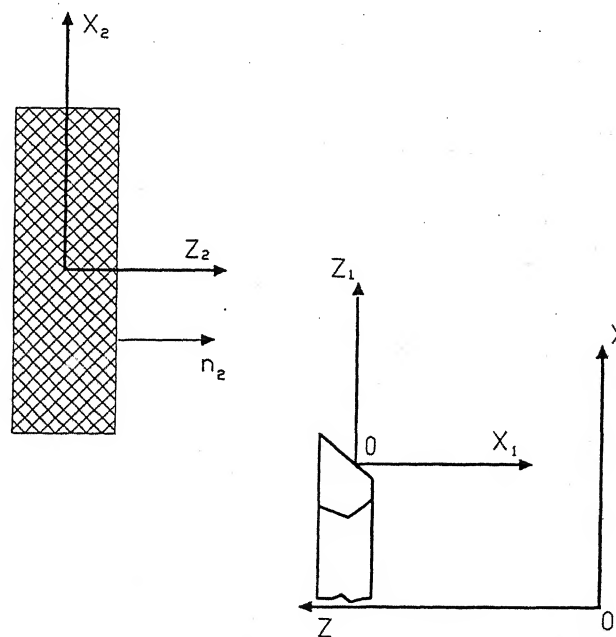


Figure 2.4(b) Grinding of Rake Face

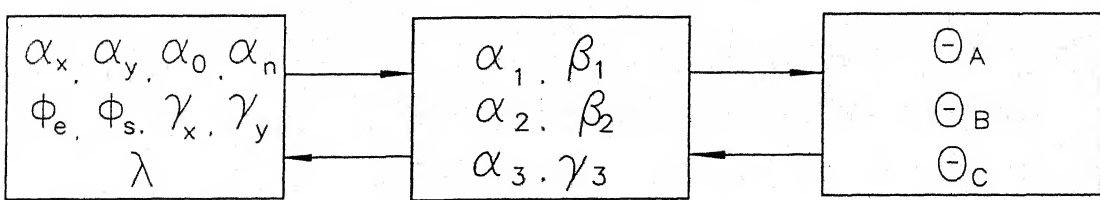
CONVENTIONAL
SYSTEMGEOMETRIC MODELLING
SYSTEMTOOL AND CUTTER
SYSTEM

Figure 2.5 Interrelationship Between Three Systems

where,

$$(-\infty \leq u_3 \leq \infty)$$

$$(-\infty \leq w_3 \leq \infty)$$

Differentiating the above equation first with respect to u_3 and then with respect to w_3 and taking the cross product of it, we get

$$\frac{\partial R}{\partial u_3} \times \frac{\partial R}{\partial w_3} = \begin{vmatrix} i & j & k \\ \cos \gamma_3 & \sin \gamma_3 \cos \alpha_3 & \sin \gamma_3 \sin \alpha_3 \\ 0 & -\sin \alpha_3 & \cos \alpha_3 \end{vmatrix}$$

$$[n_1] = \begin{bmatrix} \sin \gamma_3 \\ -\cos \gamma_3 \cos \alpha_3 \\ -\cos \gamma_3 \sin \alpha_3 \end{bmatrix}$$

$$[n_2] = \begin{bmatrix} 0 \\ 0 \\ 1 \end{bmatrix}$$

Substituting the above values in equation (2.9), we get

$$\theta_B = \tan^{-1} \left[\frac{\tan \gamma_3}{\sin \alpha_3} \right] \quad (2.14)$$

$$\theta_A = -\sin^{-1} (\cos \gamma_3 \cos \alpha_3)$$

2.7 Interrelationship Between the Three Systems.

The forward and inverse relationship between the conventional angles and the grinding angles of a single point cutting tool has already been established [9]. Now, given the setting angles θ_c , θ_B , θ_A , the grinding angles (α_1 , β_1 , α_2 , β_2 , α_3 , γ_3) are found out by using the above equations (2.9, 2.11, 2.14) we get,

For the principal flank :

$$\begin{aligned}\beta_2 &= -\theta_B \\ \alpha_2 &= -\theta_A\end{aligned}\tag{2.15}$$

For the auxiliary flank :

$$\begin{aligned}\beta_1 &= -\theta_B \\ \alpha_1 &= -\theta_A\end{aligned}\tag{2.16}$$

And for rake face :

$$\begin{aligned}\gamma_3 &= -\sin^{-1}(\sin \theta_B \cos \theta_A) \\ \alpha_3 &= \sin^{-1} \left[\frac{\tan \gamma_3}{\tan \theta_B} \right]\end{aligned}\tag{2.17}$$

Similarly , the conventional angles can also be found out from the given setting angles θ_A , θ_B , θ_c by using the forward and inverse relationship between the conventional angles and the grinding angles. Thus, if the angles from one system are given, the corresponding angles from the other two systems can be found out using the relationships between them as shown in Figure(2.5).

Chapter 3

Geometric Modeling of Helical Flutes

3.1 Introduction

The extensive use of fluted cutting tools in practice has led to the study of 3-dimensional geometry of these tools. Various kinds of fluted cutting tools used in manufacturing are twist drills, reamers, broachers, end-mills etc. Geometry of these cutting tools is studied in two parts, namely fluted shank and end geometry. The study of 3-dimensional geometry of such tools is important from grinding and sharpening point of view.

The geometric definition of the helical path along different objects such as cylinder, cone, hemisphere is given in section 3.2. The cross sectional geometry of the fluted shank is studied in section 3.3. If this cross section is swept along different helical paths, then we get the fluted surface as described in section 3.4. Then the end surface geometry of the fluted tools is studied in section 3.5. And finally the integrated geometry of the fluted shank and end part of the tool is considered in section 3.6.

3.2 Geometric Definitions of helical paths

3.2.1 Cylinder

The helical path along cylinder is shown in Figure 3.1(a). The mathematical definition of this helix is given as

$$\begin{aligned}x &= r \cos \theta \\y &= r \sin \theta \\z &= \frac{p\theta}{2\pi}\end{aligned}\tag{3.1}$$

where

$$0 \leq \theta \leq \frac{2\pi}{p} h$$

p is the pitch of the helix and h is the height of the cylinder.

3.2.2 Cone

The helical path along a frustum of a cone is shown in Figure 3.1(b). Two cases are considered, when $r_1 > r_2$ and $r_1 < r_2$. The helix along this path is defined as

$$\begin{aligned}x &= r \cos \theta \\y &= r \sin \theta \\z &= \frac{p\theta}{2\pi}\end{aligned}\tag{3.2}$$

and

$$r = r_1 + \frac{(r_2 - r_1)(h - z)}{h}$$

where

$$0 \leq \theta \leq \frac{2\pi}{p} h$$

r_1 and r_2 are two end radii of the frustum of a cone.

3.2.3 Hemisphere

The helical path along the spherical part is given by the following mathematical definition.(Figure 3.1(c).)

$$\begin{aligned}x &= r \cos \phi \cos \theta \\y &= r \cos \phi \sin \theta \\z &= r \sin \phi\end{aligned}\tag{3.3}$$

where,

$$0 \leq \phi \leq \pi / 2$$

$$0 \leq \theta \leq 2\pi$$

Relation between ϕ and θ is given by

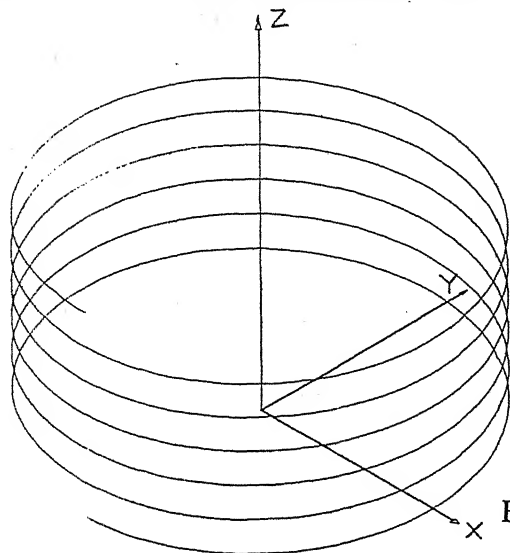


Figure 3.1(a) Helical Path along Cylinder

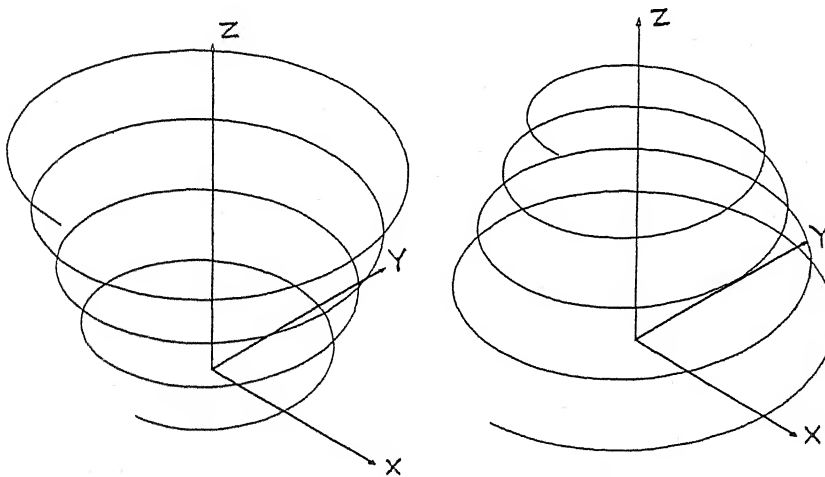


Figure 3.1(b) Helical Path along Cone

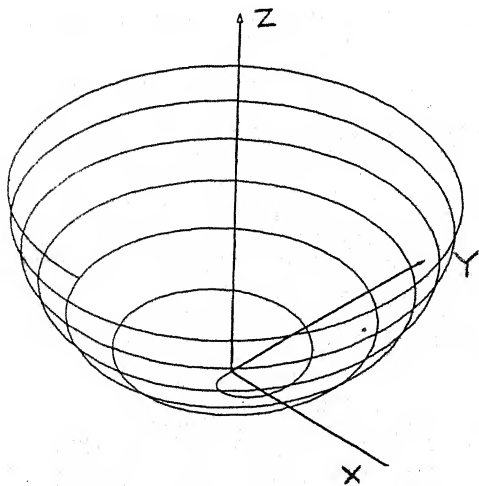


Figure 3.1(c) Helical Path along Hemisphere

$$\phi = \tan^{-1} \left[\frac{p}{r} \frac{\theta}{2\pi} \right]$$

3.2.4 Cylinder and hemisphere

Here the hemisphere is kept at the end of the cylinder. The helical path along this combination is shown in Figure 3.1(d). The helical path is defined same as in Section 3.2.1 and 3.2.3. Here the important thing is to ensure the continuity of the helix from cylinder to hemisphere which is maintained by controlling the value of θ .

3.3 Section Geometry of the Fluted Tool

Figure 3.2 shows the sectional geometry of the four fluted end-mill. For defining this section the input parameters are the rake angle (α_3), primary clearance angle (α_1), secondary clearance angle (α_2), land widths (l_1, l_2, l_3) and flute radii (r_1, r_2, r_3). With this input we can calculate the points p_1, p_2, p_3, p_6 and p_7 using simple mathematical relations. The curve portion is divided into three circular arcs. Using the condition of tangency the center points for these arcs are found out. From this information points p_5 and p_4 are found out and then they are joined to get a smooth curve segment. Thus the entire profile is defined in parametric form. Then it is rotated to get the desired cross-section of four fluted end-mill.

3.4 Fluted surface Definition of Shank

Once we get the cross-sectional profile then the fluted surface is obtained by sweeping the profile and simultaneously advancing it along the z axis. The helix angle remains constant on the fluted shank.

The sectional profile in x-y plane is parametrically defined as

$$W(u) = \begin{bmatrix} f_1(u) \\ f_2(u) \\ 0 \end{bmatrix} \quad (3.4)$$

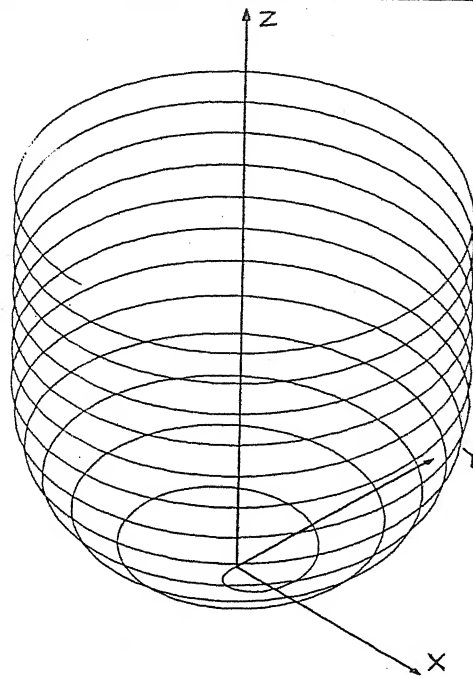


Figure 3.1(d) Helical Path along Cylinder and Hemisphere

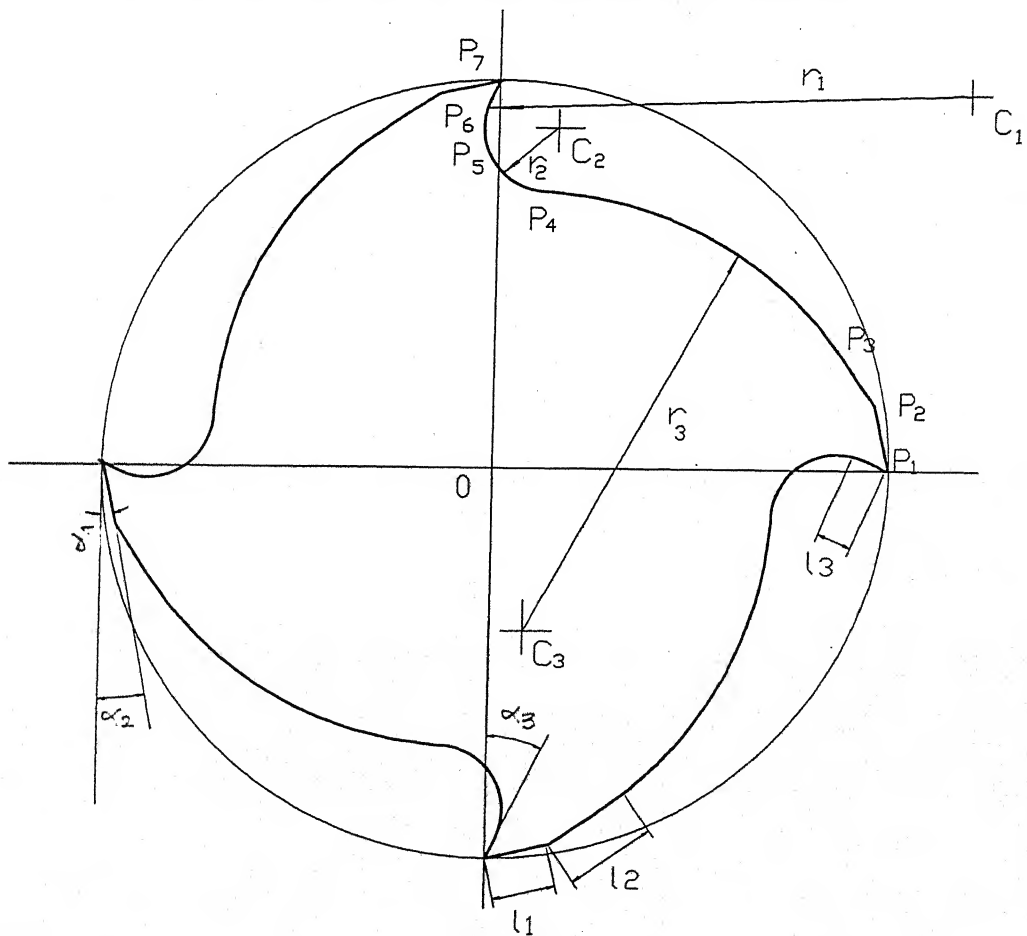


Figure 3.2 Cross-sectional Geometry of Four Fluted Tool

When this cross-section is rotated and simultaneously advanced about z axis then the helix surface is obtained which is given by

$$W(u, v) = \begin{bmatrix} f_1(u) \cos v - f_2(u) \sin v \\ f_1(u) \sin v + f_2(u) \cos v \\ \frac{H}{2\pi} v \end{bmatrix} \quad (3.5)$$

where,

H is the lead of the helix.

3.5 End Surface Geometry

The most important thing is to obtain the end surface geometry of a fluted tool. For example, in case of ball end-mill each flute lies on the surface of hemisphere, and is ground with a constant helix lead. The radius of the ball in x-y plane reduces, as we go towards the ball tip in the axial z direction. Due to this, the local helix angle varies along the cutting flute. The surface geometry on the ball part is obtained as follows.

We have already seen in Section 3.2.3 the definition of the helical path along the hemisphere. Here the cross section of the ball part is a function of z, which varies from 0 at the tip of ball part to R at the meeting of ball and shank boundary, where R is the radius of the shank portion. The radius of cross-section at any instance z, is given by

$$r(z) = \sqrt{2Rz - z^2}$$

where,

$$z = \frac{\text{ball_angle}}{2\pi} \text{pitch} \quad (3.6)$$

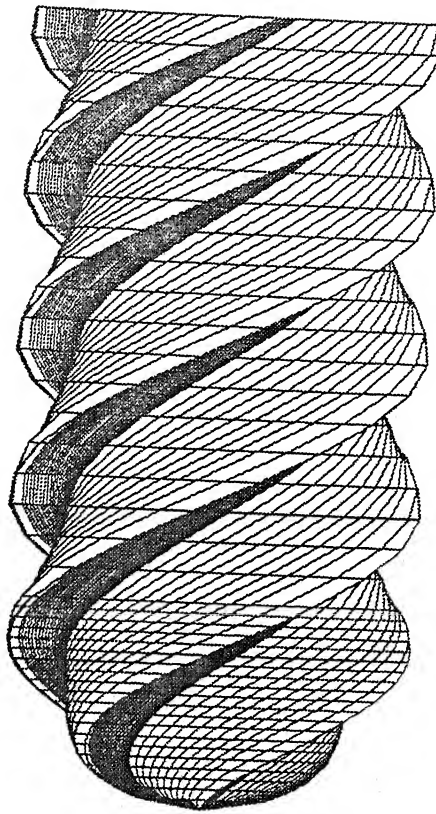


Figure 3.3 Surface Model of End-mill with Ball End

$$0 \leq ball_angle \leq \frac{R}{p} 2\pi$$

Then the ratio by which the cross-section is reduced while going towards the tip of the ball end-mill is given as

$$ratio = \frac{r(z)}{R} \quad (3.7)$$

Using this ratio in the equation(3.5), we find out the fluted surface on the ball part.

Similarly for the cone, the fluted surface is obtained. Here the radius of cross-section $r(z)$ is given by

$$r(z) = \frac{Rz}{h} \quad (3.8)$$

where,

h is the height of the cone.

3.5 Integrated Tool Geometry

First we defined the helical path over different objects such as cylinder, cone and hemisphere and this concept is used afterwards to find the fluted surface of the tool. Then we defined the cross-sectional geometry of the fluted tool. This cross-sectional profile when rotated and simultaneously swept along z axis, we get the fluted surface on shank portion and the end part separately.

Now, it is important to find the fluted surface along the tool as a whole, including the shank part and the end geometry. Here the continuity along the boundary of shank and end part is required to maintain. This continuity is obtained by controlling the value of angle θ along the z axis. Figures 3.3(a) and 3.3(b) shows the integrated tool geometry of ball end-mill and the end-mill with conical end, having four flutes.

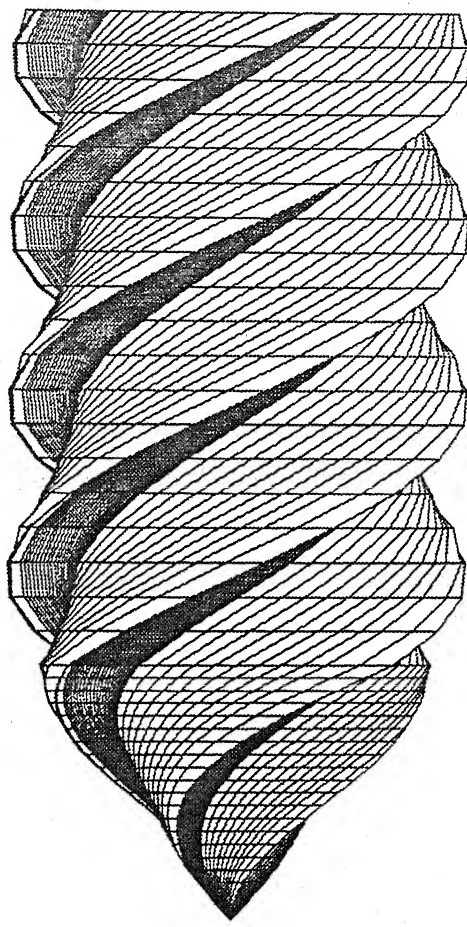


Figure 3.4 Surface Model of End-mill with Conical End

The value of θ at the start of ball tip is 0 and θ_{end} at the end of ball portion is given by

$$\theta_{end} = \frac{height}{pitch} \times 2\pi \quad (3.9)$$

Now, the value of θ at the start of end-mill portion is equal to θ_{end} . And thus the continuity of fluted surface is maintained from ball part to end-mill part.

3.7 Derivation of the Cross-sectional Profile

The section geometry of the fluted tool is described in Section 3.3. Here we will see how to obtain the cross-sectional profile. It is divided into six segments. Three segments corresponds to three land widths and three circular arcs are used to get a smooth curve segment. The input parameters are primary (α_1) and secondary (α_2) clearance angles, rake angle (α_3), land widths (l_1, l_2, l_3), flute radii (r_1, r_2, r_3), radius of the shank(r) and number of flutes(N).

The seven points ($p_1 - p_7$) and the three center points ($c_1 - c_3$) of the profile, taking origin as (0,0) are given as,

$$p_1(x) = r$$

$$p_1(y) = 0$$

$$p_2(x) = r - l_1 \sin \alpha_1$$

$$p_2(y) = l_1 \cos \alpha_1$$

$$p_3(x) = r - l_1 \sin \alpha_1 - l_2 \sin \alpha_2$$

$$p_3(y) = l_1 \cos \alpha_1 + l_2 \cos \alpha_2$$

$$p_7(x) = 0$$

$$p_7(y) = r$$

$$p_6(x) = -l_3 \sin \alpha_{31}$$

$$p_6(y) = r - l_3 \cos \alpha_3$$

(3.10)

$$c_1(x) = [r - l_1 \sin \alpha_1 - l_2 \sin \alpha_2] - r_1 \sin\left(\frac{\pi}{2} - \alpha_2\right) \quad (3.11)$$

$$c_1(y) = [l_1 \cos \alpha_1 + l_2 \cos \alpha_2] - r_1 \cos\left(\frac{\pi}{2} - \alpha_2\right)$$

$$c_3(x) = [-l_3 \sin \alpha_3] + r_3 \sin\left(\frac{\pi}{2} - \alpha_3\right) \quad (3.12)$$

$$c_3(y) = [r - l_3 \cos \alpha_3] - r_3 \cos\left(\frac{\pi}{2} - \alpha_3\right)$$

Using the condition of tangency between three arcs, we can see that the points p_5 , o and c_1 are collinear and points p_4 , o and c_3 are also collinear. With this condition we find out first the angles *theta* and *theta*₁ and center c_2 and points p_4 , p_5 as follows:

$$\begin{aligned} c_2(x) &= c_1(x) + r_1 \cos(\text{theta}_1) - r_2 \cos(\text{theta}_1) \\ c_2(y) &= c_1(y) + r_1 \sin(\text{theta}_1) - r_2 \sin(\text{theta}_1) \end{aligned} \quad (3.13)$$

$$\begin{aligned} p_4(x) &= r_2 \cos(\pi + \text{theta}) + c_2(x) \\ p_4(y) &= r_2 \sin(\pi + \text{theta}) + c_2(y) \end{aligned} \quad (3.14)$$

$$p_5(x) = r_2 \cos(\text{theta}_1) + c_2(x)$$

$$p_5(y) = r_2 \sin(\text{theta}_1) + c_2(y)$$

Thus joining the points ($p_1 - p_7$) we get the part of a profile. By rotating this profile we get the complete cross-sectional profile for the four fluted tool. Similarly we can get the profile for different number of flutes.

Chapter 4

Grinding of Fluted Tools

4.1 Grinding of Cutting Tools

In Chapter 2 we obtained the setting angles required for grinding and sharpening of a single point cutting tool. Similarly the setting angles required for the grinding of fluted surfaces are obtained in this Chapter. In order to carry out this grinding process we require minimum five to six-axis CNC tool and cutter grinder.

CNC tool and cutter grinder was introduced in 1977 and became quite capable of producing and regrinding all the basic round shank fluted cutting tools. CNC tool grinders are simpler to operate and the software requires data input such as clearance angles, rake angle, land widths, flute radius, number of flutes, diameter of shank etc. for all fluted cutting tools. Operators can enter operating parameters and tool geometry with less time and trouble. And Pentium, 486, or other fast computer chips calculate the paths of the tools and grinding wheels in seconds rather than minutes.

CNC tool and cutter grinding produces more consistent tools than manual grinding and is the only reliable way to grind matched sets of identical cutters. Diameters, angles, and lengths can be held more accurately than an expert toolgrinder can produce consistently on a good manual tool grinder. CNC grinding is much faster than manual tool grinding in part because it operates under flood coolant in an enclosed cabinet, maximizing the speeds employed with the diamond wheels without burning the tools. Speeds and feeds in end-milling may be raised 10 to 35 % over those used with manually ground tools. It is also possible to achieve more regrinds per tool with CNC grinding because all the teeth were initially ground more uniformly and thus wore evenly.

Some of the five and six axis CNC grinding machines are shown in Figure 4.1. The five axis **Walter Helitronic Power** introduced in 1994 is shown in Figure 4.1(a).

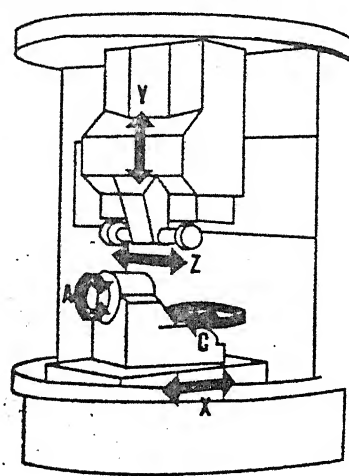


Figure 4.1(a) Five-axis Walter
Helitronic Power CNC Tool Grinder

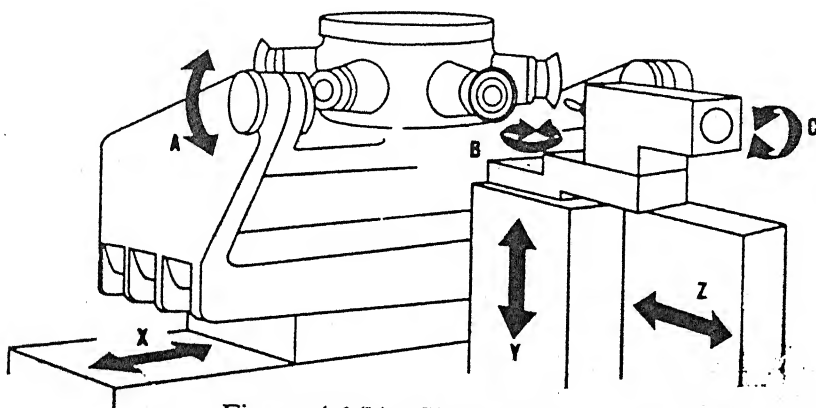


Figure 4.1(b) Six-axis Ewamatic 106 CNC Tool Grinder

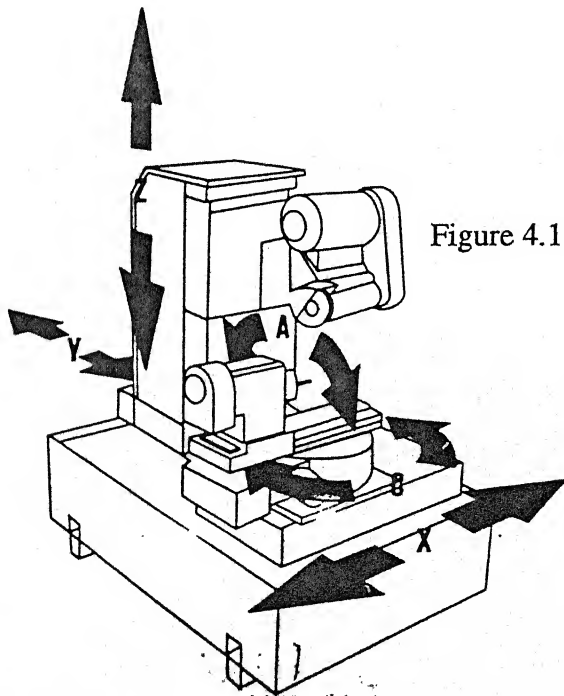


Figure 4.1(c) Five-axis Huffman HS 155
CNC Tool Grinder

The compact machine is fast and rigid and used for grinding end mill. The machine's work envelope consist of 300mm grind diameter and tool length of 280mm. The six axis Ewamatic 106 CNC tool grinder from Ewag Corp. used for grinding fluted tools is shown in Figure 4.1(b). It has six grinding spindles arranged in a circle and each spindle is capable of carrying up to three wheels. The machine grinds tools of diameter up to 25mm. The spindle speed range is 2000 to 12,000 rpm. For controlled automatic production of tools, a 3-D measuring system is mounted on the grinding head. The five axis Huffman HS 155 CNC grinder used for ball end-mill grinding is shown in Figure 4.1(c).

4.2 Rake Face Grinding

The important features of ball end-mill cutter are two clearance angles, namely primary and secondary clearance angles and rake angle. Here the grinding of flute, rake and clearance surfaces is considered separately.

Rake face is ground with a dish type wheel as shown in the Figure 4.2. The tool axis needs to be offset by

$$h = \frac{D}{2} \sin \alpha_3 \quad (4.1)$$

where,

D is the diameter of the shank and α_3 is the rake angle.

Now, we will find out the setting angles required for grinding the rake face.

The equation of the rake surface is given as

$$w(u, v) = \begin{bmatrix} f_1(u) \cos v - f_2(u) \sin v \\ f_1(u) \sin v + f_2(u) \cos v \\ cv \end{bmatrix} \quad (4.2)$$

where,

$$f_1(u) = x_1 + (x_2 - x_1)u$$

$$f_2(u) = y_1 + (y_2 - y_1)u$$

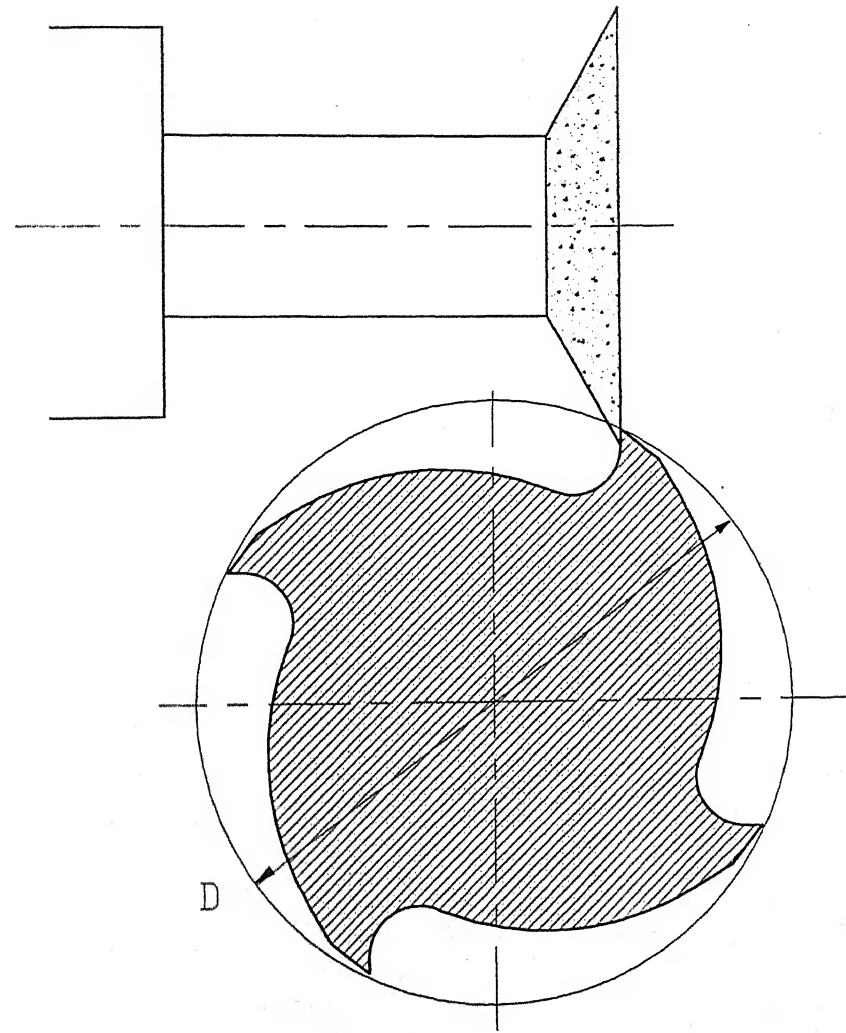


Figure 4.2 Grinding of Rake Face

$$c = \frac{\text{lead}}{2\pi}$$

The coordinates of the points $P_7(x_1, y_1)$ and $P_6(x_2, y_2)$ are known.

let

$$x_2 - x_1 = X \quad \text{and} \quad y_2 - y_1 = Y$$

Substituting these values in the equation (4.2) we get

$$w(u, v) = \begin{bmatrix} (x_1 + Xu)\cos v - (y_1 + Yu)\sin v \\ (x_1 + Xu)\sin v + (y_1 + Yu)\cos v \\ cv \end{bmatrix} \quad (4.3)$$

To find the normal on the rake face, we first differentiate the equation (4.3) with respect to u and then with respect to v and taking their cross product we get,

$$\frac{\partial \vec{R}}{\partial u} \times \frac{\partial \vec{R}}{\partial v} = \begin{vmatrix} i & j & k \\ X\cos v - Y\sin v & X\sin v + Y\cos v & 0 \\ -(x_1 + Xu)\sin v - (y_1 + Yu)\cos v & (x_1 + Xu)\cos v - (y_1 + Yu)\sin v & c \end{vmatrix} \quad (4.4)$$

Let $[n_1]$ be the normal vector acting on the rake surface.

$$[n_1] = \begin{bmatrix} c(X\sin v + Y\cos v) \\ -c(X\cos v - Y\sin v) \\ X^2 + Y^2 \end{bmatrix} \quad (4.5)$$

In order to position the tool with respect to grinding wheel and to satisfy the grinding principle, following transformations are successively carried out,

- 1) Rotation about Y axis through an angle ' θ_B '
- 2) Rotation about X axis through an angle ' θ_A '

We get the following equation,

$$[n_2] = [n_1] [R_{y,\theta_B}] [R_{x,\theta_A}] \quad (4.6)$$

where,

$[n_2]$ =normal acting on the grinding wheel surface.

Performing the algebra involved in the above equation we get the values of angle θ_B and θ_A as

$$\theta_A = \sin^{-1}[c(Y \sin v - X \cos v)] \quad (4.7)$$

$$\theta_B = \tan^{-1}\left[\frac{-c(X \sin v + Y \cos v)}{X^2 + Y^2}\right]$$

Grinding the Ball part

In the equation (4.2) angle v is a variable and for ball part it varies between the value 0 and θ_{end} . Where ,

$$\theta_{end} = \frac{\text{height}}{\text{pitch}} 2\pi$$

And the x and y coordinate of this equation (4.2) are required to multiply by a *ratio* given by,

$$\text{ratio} = \frac{r(z)}{R}$$

where, $r(z)$ is cross sectional radius of ball at distance z and is given by,

$$r(z) = \sqrt{2Rz - z^2}$$

and

$$z = \frac{\nu}{2\pi} pitch$$

Grinding the end mill portion

While grinding the end-mill portion the angle ν varies from the value of θ_{end} , where θ_{end} is the end angle of the ball part. The equation used for the end-mill surface remains same as equation (4.2). Here the angle ν varies linearly, as the helix angle remains constant throughout the end-mill portion.

4.3 Clearance Face Grinding

The clearance faces are ground either with the cup face of a grinding wheel or at the periphery of a straight wheel as shown in Figure 4.3. In both the cases the offsets are given by

$$h = \frac{D}{2} \sin \alpha \quad (4.8)$$

where,

α is the clearance angle, h is the offset from grinding wheel axis and D is the cutter diameter.

For finding the setting angles θ_B and θ_A , same procedure described above is used. Only the values of $f_1(u)$ and $f_2(u)$ will change accordingly. For primary clearance surface these values are given by the coordinates of points p_1 and p_2 and for secondary clearance surface they are given by points p_2 and p_3 . Hence the same equation (4.7) can be used for finding the setting angles θ_B and θ_A .

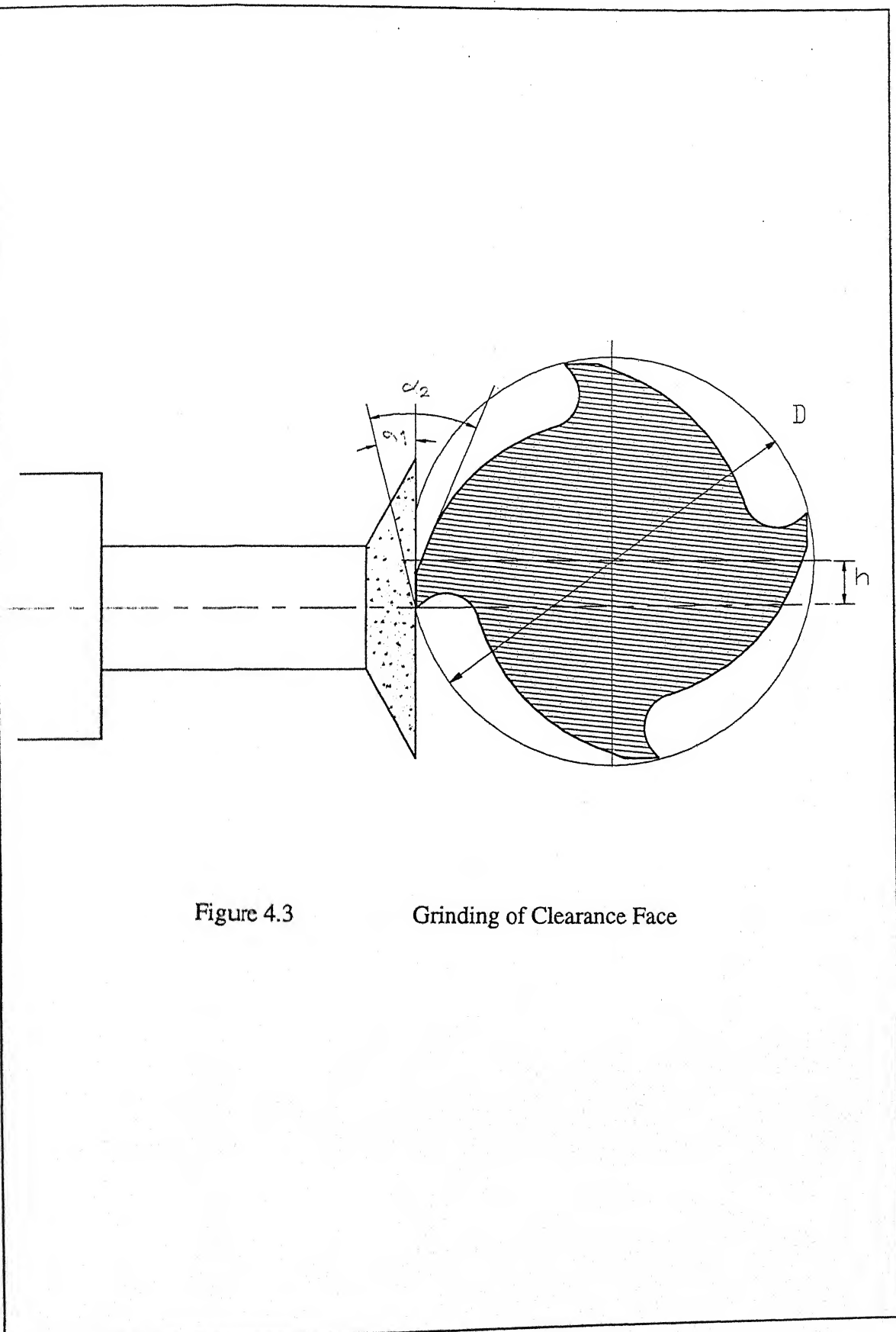


Figure 4.3 Grinding of Clearance Face

4.4 Some Observations

In the foregoing derivations, we take, the normal of the wheel face as [0 0 1] with respect to the global coordinate system. In practice, the orientation of the wheel face may not necessarily be parallel to the x-o-y plane. In such a situation the normal vector will not be [0 0 1]. However the specific orientation of the normal vector can be established based on the inclined / oblique orientation of the wheel face with respect to the global coordinate system. It should be kept in mind, however, that the grinding principle between the wheel face and cutting face remains the same.

When the clearance surface is ground with the periphery of a straight wheel, a concave land is produced. By increasing the wheel diameter, the concavity can be reduced. To reduce the possibility of burning of edges, cup wheels are swiveled in reference to the direction of wheel travel to ensure that only one side of the wheel face contacts the cutter.

Conclusions

5.1 Summary of Technical work

The primary goal of present work is to develop appropriate selection of geometric modeling for the design of single point and fluted cutting tools. The present literature relies heavily on specifying the geometries of cutting tools using the approach of projective geometry. In other words the orientation of different cutting planes or cutting surfaces are specified by taking several auxiliary sections. The sectional views indicates the inclinations of the cutting edges. These inclinations are denoted by means of different angles such as the rake angle, clearance angle etc. Such an approach was acceptable in the past since the ability of design engineer to specify the orientation of cutting surfaces was limited to 2-D cartesian coordinate frame. However the recent developments in the field of geometric modeling, computational geometry and conjugate geometry enable us to now define the cutting faces as biparametric planar surfaces. The flutes cutting surfaces can be represented as biparametric helicoidal surfaces. This concept provides a geometric definition which can be used very effectively for generating the appropriate data for grinding or resharpening of cutting tools.

Chapter 1 reviews the different types of Nomenclatures as well as the literature available in the field of design of cutting tools. The goals of the present work have been outlined in this chapter. We wish to state that all the goals have been achieved successfully. Correction in the inverse formula for finding the grinding angles is made in chapter 2. Also the method for finding the setting angles for grinding and sharpening is discussed and the interrelationship among the three systems for cutting tools is established. Chapter 3 focuses on the development of the geometric model for the fluted cutting tools such as end-mill with hemisphere and cone as the end geometry. Chapter 4 discusses the methodology of grinding the cutting surfaces such as rake and clearance of the fluted

cutting tools. These surfaces are ground using a grinding wheel, in the form a frustum of a cone.

The above said concepts are developed as a software module which can run in the environment of AutoCAD-Release 14 (Windows version). The codes are in Visual C++, using ADSRX libraries. This gives us the better visualization of the results of the mathematical developments, which were discussed in the previous chapters. Photographs of the fluted cutting tools rendered in 3D-Studio are given in Figures 5.1 and 5.2.

Not to stop just with theoretical studies, the work has been extended to advanced manufacturing system such as Rapid Prototyping process. The end-mill cutter and the extruder screws are taken as examples. The solid modeling was done using "Pro-engineer" Software, the slicing was performed using the Quick-Slice software and the FDM-1650 RP machine was used to build the rapid-prototype model . (Figures 5.3 -5.6)

5.2 Suggestions for Further Work

The methodology developed in the previous chapters can be used for the modeling of twist drill for grinding and sharpening.

There is a need for defining the end geometry of various fluted cutting tools. In the present work, end geometry of ball end-mill and conical end-mill is discussed. Similarly the modeling of the fluted tools with other end geometries can be done.

Development of user-friendly software for the purpose of grinding of single point and fluted cutting tools could be done. The features of this software would include menu-driven, graphical display, post processing for various types of CNC machines etc.

There are other cutting tools apart from single point and fluted cutting tools, which can be modeled on similar lines described in this work

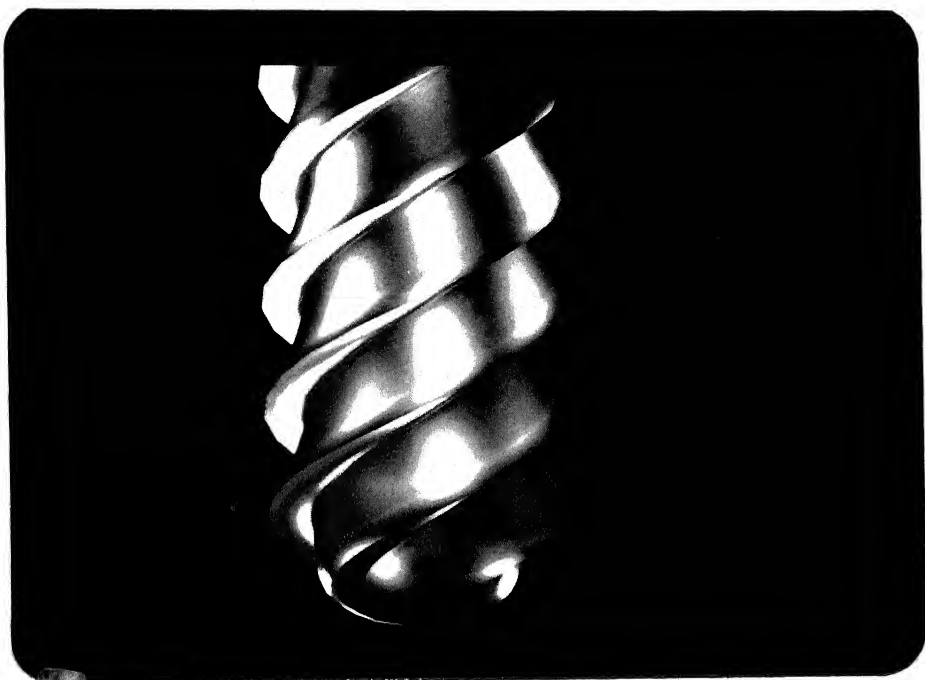


Figure 5.1

End-mill with Ball End

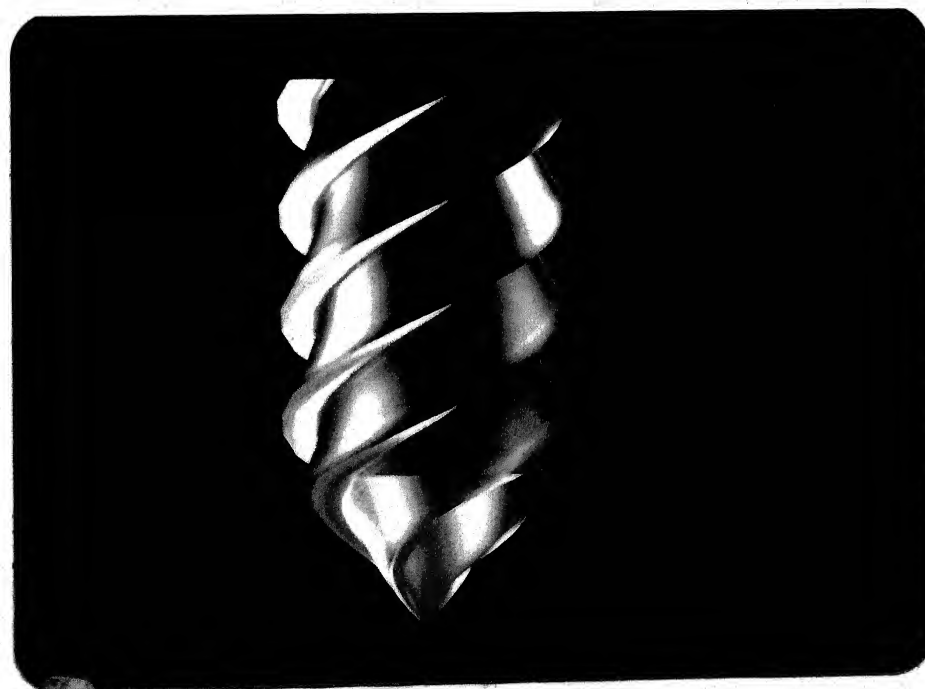


Figure 5.2

End-mill with Conical End

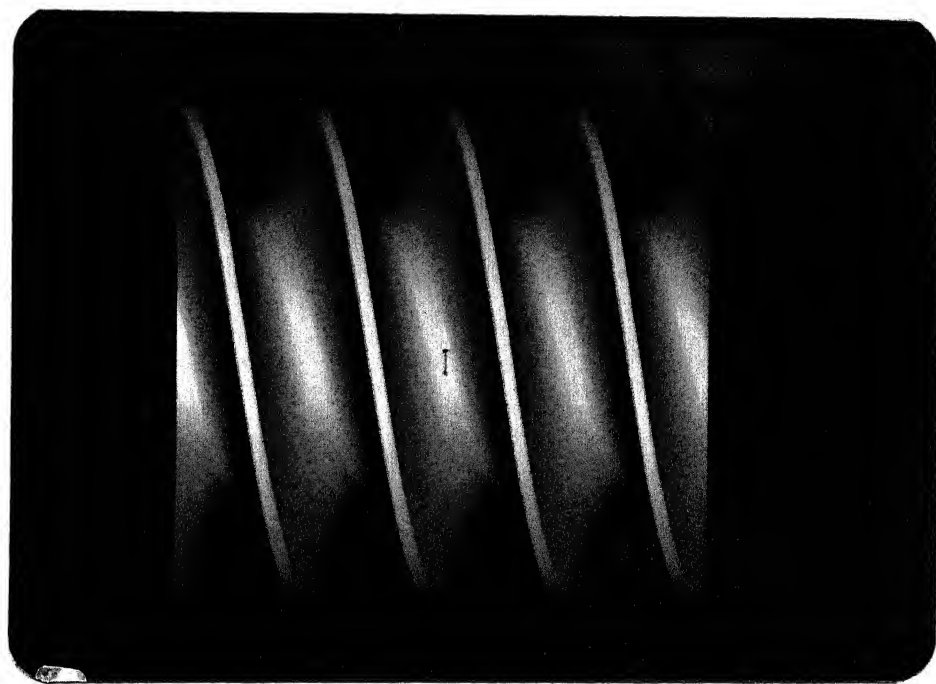


Figure 5.3 Extruder Screw

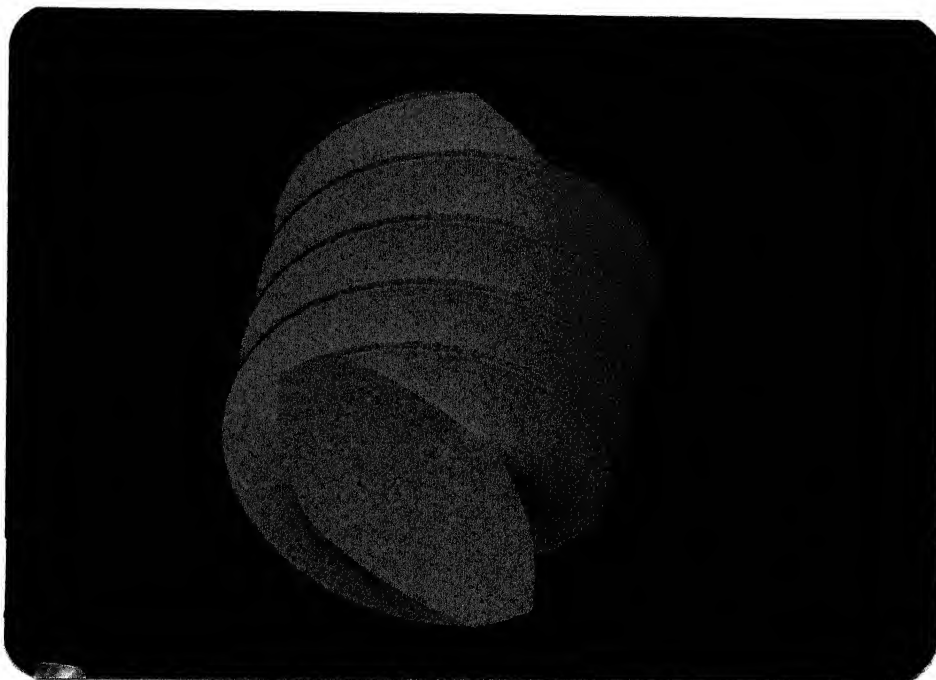


Figure 5.4 Extruder Screw

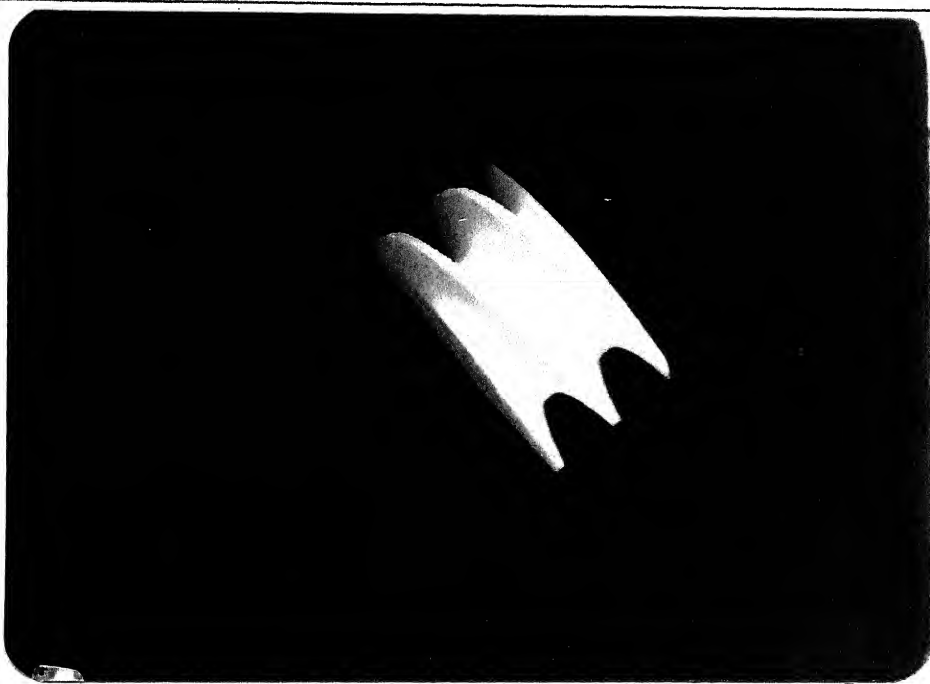


Figure 5.5

Rapid Prototype Model of Extuder Screw

References

[1] Altintas Y., Lee P., (1996), "A General Mechanics and Dynamics Model for Helical End Mills ", *Annals of CIRP*, Vol. 45, No 1, pp. 59-64

[2] Altintas Y., Yucesan G.,(1996), "Prediction of Ball End Milling Forces", *Journal of Engineering for Industry*, Vol. 118, No 1, pp. 95-103

[3] Altintas Y., Lee P., (1996), "Prediction of Ball End Milling Forces From Orthogonal Cutting Data", *International Journal of Machine Tools Manufacturing*, Vol. 36, No. 9, pp. 1059-1072

[4] Bhattacharya A. (1984), Metal Cutting, Theory and Practice, Central Book Publishers, Calcutta, pp. 33-113

[5] Fujii, S., Devries, M.F., Wu, S.M., (1972), "Analysis and design of the drill grinder and evaluation of the grinding parameters", *Trans of ASME, Journal of Engg for Industry*, Vol. 94, No 4, pp. 1157-1163

[6] Lin C., Kang, S.K., Ehmann, K.F.,(1995), "Helical Micro-drill Point design and grinding", *Trans. of the ASME, Journal of Engg for Industry*, Vol 117, pp. 277-287

[7] Mortenson M.E., (1985), Geometric Modeling, John Wiley & Sons, Inc. , New York, pp 151-234

[8] Popov s., Dibner L. & Kamenkovich A., (1984), sharpening of Cutting Tools, Mir Publishers, Moscow, pp 156-200

CENTRAL LIBRARY
I.I.T., KANPUR
Call No. A 124439

- [9] Rajpathak T. S., (1996), "Geometric Modeling of Single Point Cutting Tools for Grinding and Sharpening", M.Tech. Thesis submitted to the Department of Mechanical Engineering , I. I. T. Kanpur, pp 12-57
- [10] Rogers.D. F & Adams J.A., (1990), Mathematical Elements of Computer Graphics, McGraw Hill Publishing Company, USA, pp 101-141
- [11] Tai Ching-Chih and Fuh Kuang-Hua (1993), "A Predictive force Model In Ball End Milling Including Eccentricity Effects", *International Journal of Machine Tools Manufacturing*, Vol. 34, No 7, pp. 959-979
- [12] Tsai, W.D., Wu, S.M., (1978), "Computer analysis of drill point geometry", *I.M.T.D.R*, Vol 19, pp. 95-108
- [13] Tsai, W.D., Wu, S.M., (1979), "A Mathematical Model for drill point design and Grinding", *Trans. of the ASME, Journal of Engg for Industry*, Vol 117, pp. 277-287
- [14] Yang Minyang and Park Heeduck, (1991), " The Prediction of Cutting Forces In Ball End Milling", *International Journal of Machine Tools & Manufacturing*, Vol. 31, No 1, pp. 45-54

Appendix A

Transformations

Transformations are used to change either the position, orientation, or the shape of an object. These transformations are applied directly to the most basic entities i.e. points, written in the matrix form, using the homogeneous system of coordinates.

A1.1 Translation

Translation refers to the change of position of a geometric object. The objects are translated in space by multiplying each and every point that makes up the entity by a geometric transformation matrix. Thus, if p is the position vector of any point, which is to be moved in X, Y, or the Z-direction through distances say l, m, or n respectively, the same could be obtained from the following equation

$$[p^*] = [p] + [T] \quad (\text{A1})$$

where the position vector is given by

$$[p] = [x \ y \ z \ 1]$$

and the transformation matrix is given by

$$[T] = \begin{bmatrix} 1 & 0 & 0 & 0 \\ 0 & 1 & 0 & 0 \\ 0 & 0 & 1 & 0 \\ l & m & n & 1 \end{bmatrix} \quad (\text{A2})$$

A1.2 Rotation

Rotational transformation is the transformation process in which an object is rotated about the coordinate axis or about an arbitrary axis in space through a certain

specific angle. To transform an object in this sense, each and every point is to be rotated about the axis. However, the rotations about the three coordinate axes are important. If a point is to be rotated in space about the Y-axis through a +ve angle β

$$[p^*] = [p][R_{y,\beta}]$$

where,

$[p^*]$ is the position vector of transformed point and

$$[R_{y,\beta}] = \begin{bmatrix} \cos \beta & 0 & -\sin \beta & 0 \\ 0 & 0 & 0 & 0 \\ \sin \beta & 0 & \cos \beta & 0 \\ 0 & 0 & 0 & 1 \end{bmatrix} \quad (\text{A4})$$

Above transformation clearly shows that a rotation about the Y-axis does not affect the Y-coordinate of the position vector of any point on the object. The rotation is considered positive in the right hand sense i.e. clockwise as one looks outward from the origin in the positive direction along the rotational axis. In a similar manner, the transformation matrices for +ve rotations about the X & Z axes are given by

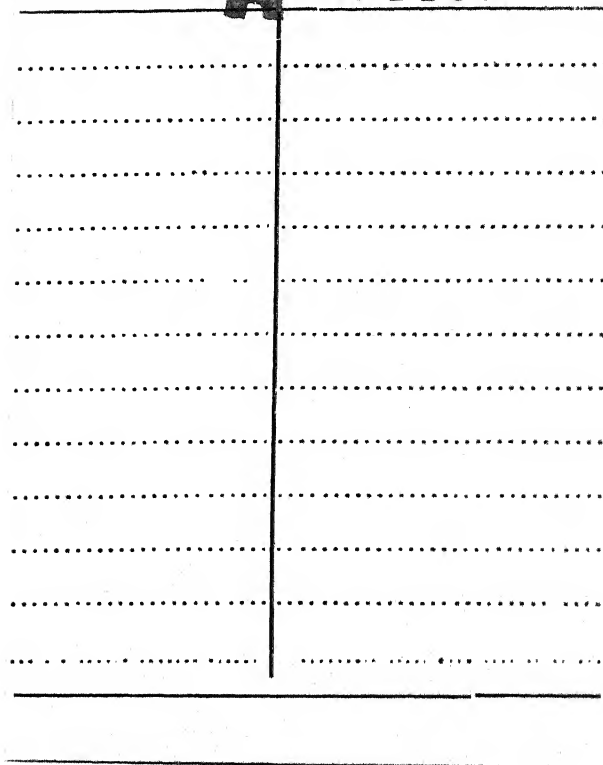
$$[R_{x,\alpha}] = \begin{bmatrix} 1 & 0 & 0 & 0 \\ 0 & \cos \alpha & \sin \alpha & 0 \\ 0 & -\sin \alpha & \cos \alpha & 0 \\ 0 & 0 & 0 & 1 \end{bmatrix} \quad (\text{A5})$$

$$[R_{z,\gamma}] = \begin{bmatrix} \cos \gamma & \sin \gamma & 0 & 0 \\ -\sin \gamma & \cos \gamma & 0 & 0 \\ 0 & 0 & 1 & 0 \\ 0 & 0 & 0 & 1 \end{bmatrix} \quad (\text{A6})$$

A 124439

Date Slip

This book is to be returned on the
date last stamped. **124439**



ME-1997-M-DEO-GEO



A124439